

Vacuum Instability in Electric Fields via AdS/CFT: Euler-Heisenberg Lagrangian and Planckian Thermalization

Koji Hashimoto^{1*} and Takashi Oka²

¹ *Department of Physics, Osaka University, Toyonaka, Osaka 560-0043, Japan*
E-mail: koji(at)phys.sci.osaka-u.ac.jp

² *Department of Applied Physics, University of Tokyo, Tokyo 113-8656, Japan*
E-mail: oka(at)ap.t.u-tokyo.ac.jp

ABSTRACT: We analyze vacuum instability of strongly coupled gauge theories in a constant electric field using AdS/CFT correspondence. The model is the $\mathcal{N} = 2$ 1-flavor supersymmetric large N_c QCD in the strong 't Hooft coupling limit. We calculate the Euler-Heisenberg effective Lagrangian $\mathcal{L}(E)$, which encodes the non-linear response and the quantum decay rate of the vacuum in a background electric field E , from the complex D-brane action in AdS/CFT. We find that the decay rate given by $\text{Im } \mathcal{L}(E)$ becomes nonzero above a critical electric field set by the confining force between quarks. A large E expansion of $\text{Im } \mathcal{L}(E)$ is found to coincide with that of the Schwinger effects in QED, replacing its electron mass by the confining force. Then, the time-dependent response of the system in a strong electric field is solved non-perturbatively, and we observe a universal thermalization at a shortest timescale “Planckian thermalization time” $\tau_{\text{th}} \sim \frac{\hbar}{k_B T_{\text{eff}}^\infty} \sim \frac{\hbar}{k_B} E^{-1/2}$. Here, T_{eff}^∞ is an effective temperature which quarks feel in the nonequilibrium state with nonzero electric current, calculated in AdS/CFT as a Hawking temperature. Stronger electric fields accelerate the thermalization, and for a realistic value of the electric field in RHIC experiment, we obtain $\tau_{\text{th}} \sim 1$ [fm/c], which is consistent with the believed value.

KEYWORDS: Vacuum decay, AdS/CFT, Schwinger effect, Holography.

*Also at *Mathematical Physics Lab., RIKEN Nishina Center, Saitama 351-0198, Japan*

Contents

1. Introduction	1
2. Review: I-V curve in holography	7
3. Vacuum instability in a holographic gapless system	11
3.1 The effective Lagrangian	12
3.2 Coincidence with Schwinger at vanishing density	14
3.3 Energy difference between the $j = 0$ and $j = j_0$ states	15
4. Vacuum instability in holographic system with mass gap	16
4.1 Critical electric field and the confining force	16
4.2 Imaginary part: coincidence with Schwinger	18
4.3 Euler-Heisenberg Lagrangian	20
5. Time-dependent process: relaxation and thermalization	22
5.1 Equations of motion and effective Hawking temperature	22
5.2 Planckian thermalization accelerated by electric fields	25
6. Conclusion and discussions	29
A. The imaginary action at zero temperature	32
B. The induced metric and the volume	33

1. Introduction

Extreme environments, such as a strong electric field, is one of the frontiers to test physical systems and to reveal new physical phenomena. Particle physics is not an exception. The physics of quantum fields in strong external electric fields, *i.e.*, “strong-field quantum field theory” has a very long history which even dates back to the development era of QED. Nevertheless, the dynamics of quantum fields and their vacuum in strong electromagnetic fields has not been understood well yet, both theoretically and experimentally.

One of the present frontiers of strong field QFT is to understand the instability of strongly interacting systems such as the confining vacuum in QCD. These theoretical researches are motivated by many experimental and natural phenomena. Famous

examples are heavy ion collisions at RHIC and LHC experiments where strong magnetic and electric fields are expected to be instantly produced [1]¹ Other examples include magnetars, neutron stars whose surface magnetic field is extremely strong and would be related to the dense hadron/quark phase inside the stars.

A particular interest is a relation between the confinement in QCD and the strong electric field. Because quarks have electric charges, a strong electric field can induce a vacuum decay at which pairs of a quark and an antiquark are produced from the vacuum to cancel the background electric field. However to estimate the threshold critical electric field, as well as to describe the physical decay process, is a difficult problem, because of several reasons; first, QCD is strongly coupled so the standard perturbative calculation does not work at low energy, and second, strong electromagnetic fields induces effective multi-photon vertices resulting in a complicated nonlinear electromagnetic effective action.

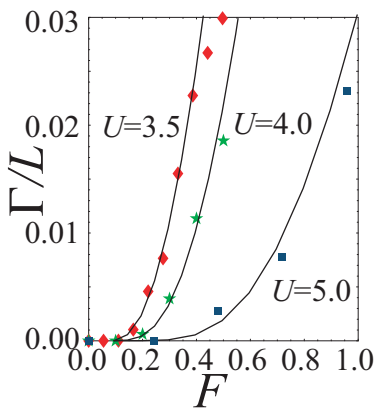


Figure 1: The ground state decay rate of the 1-dimensional Mott insulator obtained numerically (dots) and analytically (solid lines) in the Hubbard model for several values of its interaction strength U [5].

Another source of our motivation comes from nonequilibrium phenomena in strongly correlated electrons in condensed matter physics [6, 7, 5, 8, 9, 10, 11, 12, 13]. The physics of strong electric field breaking the vacuum is nothing but a famous notion known as dielectric breakdown in material science. The Mott insulator, which hosts high T_c superconductivity when doped (=carriers are added) in cuprates, is a state in which the motion of electrons are frozen due to strong Coulomb repulsion. In order to realize ultrafast control of the Mott metal-insulator transition, as well as superconductivity, its nonequilibrium response in strong electric field is being intensively studied. An example of the decay rate of the Mott insulating ground state is shown in Fig. 1, and in fact one can observe the threshold behavior with a critical electric field.

The renowned method for analyzing strongly coupled system, such as QCD, is the AdS/CFT correspondence (also called holography or gauge/gravity duality) [14, 15, 16]. This is a well-developed tool in string theory which enables us to analyze strongly coupled QCD analytically. In this paper, we apply the gauge/gravity duality to a certain strongly coupled QCD-like gauge theory, and analyze the instability caused by a strong electric field. The theory is a toy model of QCD — $\mathcal{N} = 2$ supersymmetric large N_c 1-flavor QCD. Using the gauge/gravity duality, we present our analytic calculations on how the instability occurs under the strong electric field, for both gapped and gapless cases (massive and massless quarks respectively), and for both time-independent and time-dependent

¹See Ref. [2] for a review on the quark gluon plasma. In this paper we concentrate on purely Maxwell electric effect on QCD-like gauge theories, and will not consider color-electromagnetic forces related to color glass condensate [3] and glasma [4].

nonequilibrium processes.

The main result of the present paper is an analytic computation of the full electromagnetic effective Lagrangian for a strongly coupled QCD-like gauge theory. In particular, the imaginary part of the effective Lagrangian shows the decay rate of the vacuum of the gauge theory. To explain the notion in more detail, here let us briefly review the case of QED.

Shortly after Dirac's theory of positron, Heisenberg and Euler [17] as well as Weisskopf [18] showed that the Dirac vacuum behaves as a dielectric, which can be polarized by electric fields. This effect can be elegantly captured by the effective Lagrangian first studied by Heisenberg and Euler [17] and later by Schwinger [19] (see Ref. [20, 21] for a review with recent developments and Ref. [6] for application in condensed matter physics.). As for QED, the one-loop effective Lagrangian is given by

$$\mathcal{L}_{\text{QED}}^{1\text{-loop}} = -i \ln \int \mathcal{D}[\psi, \bar{\psi}] \exp \left[i \int d^4x \bar{\psi} (i\mathcal{D} - m) \psi \right] / V \quad (1.1)$$

$$= -i \ln \det(i\mathcal{D} - m) / V, \quad (1.2)$$

where the Dirac operator is $\mathcal{D} = \gamma^\mu (\partial_\mu + ieA_\mu)$, A_μ is a fixed external gauge potential with its field strength tensor $F_{\mu\nu} = \partial_\mu A_\nu - \partial_\nu A_\mu$, m the electron mass and V is the spacetime volume. The effective Lagrangian serves as a generating function for non-linear responses of the vacuum, *e.g.*, vacuum polarization, light-light scattering. The polarization induced by the static electric field E is related to the real part of the effective Lagrangian

$$P(E) = \frac{\partial \text{Re}\mathcal{L}}{\partial E}. \quad (1.3)$$

An interesting observation is that the effective Lagrangian has an imaginary part

$$\mathcal{L} = \text{Re}\mathcal{L} + i\Gamma/2. \quad (1.4)$$

The effective Lagrangian is related to the vacuum-to-vacuum amplitude via [5]

$$\langle 0|U(t)|0\rangle = e^{i\mathcal{L}vt}, \quad (1.5)$$

where v is the spatial volume, $U(t)$ is a time-evolution operator with external fields, $|0\rangle$ is the original vacuum state (with no external fields). Thus, Γ gives the vacuum decay rate. For QED, the imaginary part is given, up to 1-loop order, by

$$\text{Im } \mathcal{L}_{\text{spinor}}^{1\text{-loop}} = \frac{e^2 E^2}{8\pi^3} \sum_{n=1}^{\infty} \frac{1}{n^2} \exp\left(-\frac{\pi m^2}{eE} n\right), \quad (1.6)$$

$$\text{Im } \mathcal{L}_{\text{scalar}}^{1\text{-loop}} = \frac{e^2 E^2}{16\pi^3} \sum_{n=1}^{\infty} \frac{(-1)^{n-1}}{n^2} \exp\left(-\frac{\pi m^2}{eE} n\right) \quad (1.7)$$

for spinor and scalar particles. The term $\exp\left(-\frac{\pi m^2}{eE}\right)$ represents a single quantum tunneling process where a pair of an electron and a hole (positron) is created from the vacuum. The threshold field, often denoted as the Schwinger limit, is given by

$$E_{\text{cr}} \sim \frac{m^2 c^3}{e\hbar} \sim 10^{16} \text{ V/cm}. \quad (1.8)$$

Experimentally, it is still not easy to produce an electric field as strong as the Schwinger limit even with the strongest lasers available.

In QCD, we expect a similar threshold electric field, since to liberate the quark and the antiquark from a meson bound state one needs an electric field which overwhelms the confining force existing between the quark and the antiquark. A similar phenomena was studied in a toy-model of confinement, namely the massive Schwinger model (1+1 dimensional QED), where the electric flux line between the electron and the positron gives a linear potential due to dimensionality providing a confining force. It was shown that when the external electric field equal the confining force, a confinement-to-deconfinement transition takes place, with massless excitation described by Coleman's half-asymptotic state [22]. Thus, it is an interesting question to study QCD near and above the critical field.

In this paper, we confine ourselves to the case of 1-flavor and at large N_c for the gauge group $SU(N_c)$, instead of the realistic QCD, to study this liberation issue. The reason is that in QCD we still have gauge-singlet observable states which are charged — charged mesons and baryons. If we consider the 1-flavor and the large N_c , there exists no charged meson, and any baryon is infinitely heavy so it is difficult to create a pair of a baryon and an anti-baryon.

The simplest example that can accommodate our interest is the $\mathcal{N} = 2$ supersymmetric QCD whose gravity dual description [23] has been studied in detail in various literature. In this paper, we shall use this supersymmetric QCD as an example to investigate the instability of the confining strongly-coupled system.

In string theory, it is predicted that pair creation of open strings should take place in the presence of electric fields [24, 25]. In the gauge/gravity setup, this leads to the pair creation of quark antiquarks via the *holographic Schwinger effect* studied by Semenoff and Zarembo [26]. However this Schwinger effect treats an instanton process which is valid at small electric field, while we are interested in strong electric fields.

The Euler-Heisenberg effective Lagrangian is defined from a partition function of a QFT in background electric fields E , *c.f.*, (1.1),

$$\mathcal{L} = -i \ln Z_{\text{QFT}}[E]/V. \quad (1.9)$$

We notice that the D-brane action, the low energy effective Lagrangian of open strings on the D-brane, is already nonlinear Dirac-Born-Infeld type [27] and it serves as an

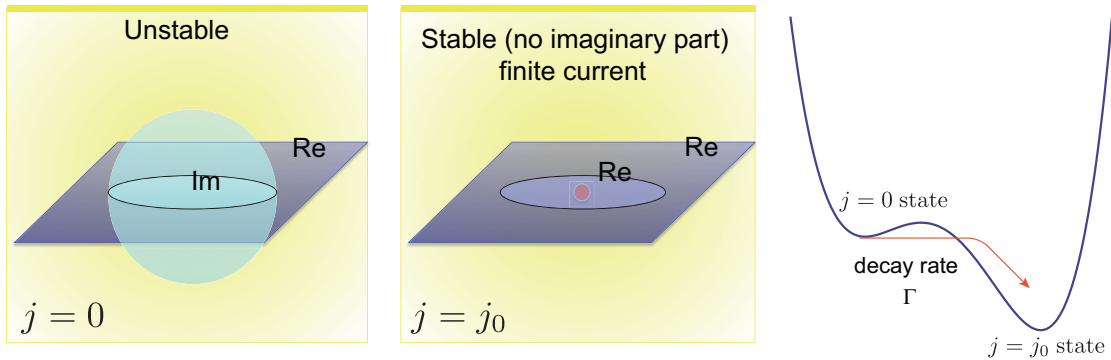


Figure 2: A schematic picture of the D7-brane in the $AdS_5 \times S^5$ geometry. The flat surface in the figure is the D7-brane on which we have a constant electric field. Left: When the field exceeds a critical value, the initial zero current solution has an effective Lagrangian with an imaginary part. This comes from a region in the D7 brane worldvolume near the D3 brane (denoted by the blue sphere). Middle: When the stable solution with non-zero current $j = j_0$ is realized, the D7-brane effective action becomes real. At the same time, an apparent horizon is formed. Right: Schematic stability diagram, where the electric field makes the initial $j = 0$ state unstable due to quantum tunneling. The system relaxes to the steady state with non-zero current.

Euler-Heisenberg Lagrangian of our supersymmetric QCD via the gauge/gravity duality. The D-brane actions are valid also for strong electric fields, so it suits our aim. More precisely, according to the gauge/gravity duality, *the Euler-Heisenberg effective Lagrangian of the $\mathcal{N} = 2$ supersymmetric $SU(N_c)$ QCD at the strong coupling limit and the large N_c limit, is simply given by the flavor D-brane effective action in a higher-dimensional curved spacetime.* When we turn on the electric field, the effective Lagrangian shows a nonlinear dependence on the field. Furthermore, we observe that when the electric field exceeds a critical value, it automatically induces an imaginary part in the D-brane action.² This gives a signal of the instability of the strongly coupled QCD.

A schematic view of the D-brane configuration is given in Fig. 2. The electromagnetic effect takes place through the charged matter field (quarks) whose dynamics is dictated by the flavor probe D-brane in the $AdS_5 \times S^5$ geometry. Once we apply the constant electric field, and when the field exceeds a critical value, a region in the D-brane worldvolume appears which gives an imaginary contribution to its effective

²For an early study of the imaginary part for a non-supersymmetric confining gauge theory in AdS/CFT, see [28].

action (the left panel of Fig. 2). After the vacuum breakdown, the system should flow to a nonequilibrium steady state with a constant electric current (the central panel of Fig. 2). The nonequilibrium steady state has been studied in previous literatures using the gauge/gravity duality. Our standpoint in this paper lies in the dynamical process starting from the unstable state in the left panel of Fig. 2.

In this paper, using the gauge/gravity duality, we find the following; For the static situation,

- We obtain the Euler-Heisenberg Lagrangian.
- We find a critical electric field to have the imaginary part, which coincides with the confining force between quarks.
- Surprisingly, the imaginary Lagrangian agrees with that of the Schwinger's calculation for QED in the strong-field expansion, via a simple re-interpretation of the electron mass by the confining potential.

In addition, since the gauge/gravity duality works also at time-dependent situations, we can study the real time dynamics when a time-dependent electric field is applied. For this dynamical case,

- We find induced time-dependent electric current and also its relaxation to a stationary current.
- The system thermalizes with a universal Planckian time $\tau_{\text{th}} \sim \frac{\hbar}{k_B T_{\text{eff}}} \sim \frac{\hbar}{k_B} E^{-1/2}$ after an abrupt introduction of the electric field.

The quantum quench on the flavor (quark) degrees of freedom has been studied in the context of AdS/CFT [29, 30], in addition to the thermalization due to the quantum quench on the bulk gluons (and the spatial volume) in AdS/CFT (see for example Refs. [31, 32, 33, 34, 35, 36, 37, 38, 39, 40]). Recently, a universal time-scale of abrupt change in parameters in AdS/CFT was reported [41]. Our universal Planckian thermalization is for a flavor quench with an abrupt changes in the electric fields.

The organization of this paper is as follows. In section 2, we briefly review the D3-D7 brane configuration in the gauge/gravity duality of the $\mathcal{N} = 2$ supersymmetric large N_c QCD, and review the steady state solution with non-zero electric current in electric fields. In section 3, we treat the gapless (massless) QCD. We evaluate the imaginary part of the Euler-Heisenberg action, and see the agreement with the standard result of the QED Schwinger effect. In section 4, we study the system with a mass gap: the massive QCD. Again we see agreement with the Schwinger effect, for large electric field expansion. Section 5 is for the time-dependent analysis, with dynamical electric current and the thermalization of the system seen in the apparent horizon in the gravity dual. The final section is devoted for discussions. In particular,

a relation to the previously-known holographic generalization of the Schwinger effect [26]³ is discussed.

2. Review: I - V curve in holography

Using gauge/gravity duality, one can analyze the full E -dependence of the current. Interestingly, in the steady state, the relation between the current j and the applied electric field E is determined by requiring that the D-brane action is real [47].⁴ Our paper concerns the imaginary part of the D-brane action (which is related to the instability) on the other hand. In this section, after presenting some basics of the gravity setup, we explain the reality condition which is used to realize the stable state.

In string theory, the simplest and best-understood system which has a charged fermion in the AdS/CFT set-ups is the renowned D3D7 system [23]. The gauge theory realized at low energy is a supersymmetric QCD-like theory. Precisely, the content of the fields consists of $\mathcal{N} = 4$ supersymmetric $SU(N_c)$ Yang-Mills theory in accompany with a $\mathcal{N} = 2$ hypermultiplet in the fundamental representation of the color $SU(N_c)$ gauge group, in 1+3 dimensional spacetime. We may consider a finite temperature system of the gauge theory. The gravity dual of the gauge theory is a D7-brane put in the AdS black hole background.

The background metric is produced by a near horizon geometry of N_c D3-branes put at a finite temperature,

$$ds^2 = \frac{R^2}{z^2} \left[- \left(1 - \frac{z^4}{z_H^4} \right) dt^2 + \left(1 - \frac{z^4}{z_H^4} \right)^{-1} dz^2 + d\vec{x}^2 \right] + R^2 d\Omega_5^2. \quad (2.1)$$

The coordinate z measures the holographic direction, and $z = 0$ corresponds to the AdS boundary. $z = z_H$ is the horizon of the black hole, so the bulk spacetime is bounded as $0 < z < z_H$. R is the AdS radius, and $d\vec{x}^2 = dx_1^2 + dx_2^2 + dx_3^2$. The temperature T and the gauge coupling constant g_{QCD} (or in other words the 't Hooft coupling constant $\lambda \equiv N_c g_{\text{QCD}}^2$) are given in terms of the geometry as

$$z_H = \frac{1}{\pi T}, \quad R^4 = 4\pi g_s N_c \alpha'^2, \quad 2\pi g_s = g_{\text{QCD}}^2. \quad (2.2)$$

Here α' is a string theory parameter given in such a way that $1/(2\pi\alpha')$ is the fundamental string tension, but will cancel out in any final results once we calculate gauge theory quantities.

The D7-brane is placed to introduce the hypermultiplet (the charged fermions). For simplicity here we consider a massless hypermultiplet (In the next section we

³Recent analyses of the holographic Schwinger effect include Refs. [42, 43, 44, 45, 46].

⁴See also Ref. [48] for a phase diagram and the metal-insulator transition. See Ref. [49] for a review of the meson sector of the D3-D7 model. For confining gauge theories, analogous analyses have been made in Refs. [50, 51, 28].

study a massive system). The hypermultiplet comes from oscillations of a string connecting the D3-brane and the D7-brane, so the masslessness corresponds to the D7-brane configuration touching the stack of D3-branes. The D7-brane action is

$$S_{D7} = -\mu_7 \int dt d^3 \vec{x} dz d\Omega_3 \sqrt{-\det [P[g]_{ab} + 2\pi\alpha' F_{ab}]}. \quad (2.3)$$

Here F_{ab} , the electromagnetic field on the probe D7-brane, plays the most important role in our paper. The external electric field determines the configuration of F_{ab} and also the electric current in the gauge theory. $\mu_7 \equiv 1/((2\pi)^7 g_s \alpha'^4)$ is the D7-brane tension, and the integration measure $dz d\Omega_3$ is for the extra 4-dimensional space which differs from the D3-brane worldvolume (our 1+3 dimensional spacetime). $P[g]_{ab}$ is the induced metric on the D7-brane.

The local gauge field appearing here in the D7-brane action in the gravity side corresponds to the global symmetry of the fermion number in the gauge theory side. If we call the fermions "quarks", this symmetry is related to the quark number (which is roughly a baryon number) in the supersymmetric QCD. Our aim is to introduce an "electric field" coupled to the charge of the quark number symmetry.⁵

For a flat D7-brane in the bulk geometry (which always solve the equations of motion for the scalar field on the D7-brane determining the shape of the D7-brane), the effective Lagrangian (which is the action divided by the spacetime volume) can be evaluated as

$$\mathcal{L} = -2\pi^2 \mu_7 \int dz \frac{R^8}{z^5} \sqrt{\xi(F_{01}, F_{0z}, F_{1z})}, \quad (2.4)$$

$$\xi \equiv 1 - \frac{(2\pi\alpha')^2 z^4}{R^4} \left[F_{01}^2 \left(1 - \frac{z^4}{z_H^4}\right)^{-1} + F_{0z}^2 - F_{1z}^2 \left(1 - \frac{z^4}{z_H^4}\right) \right]. \quad (2.5)$$

Note that here and in the following we write spacetime Lagrangian density rather than the action. The factor $2\pi^2 = \text{Vol}(S^3)$ results from the $d\Omega_3$ integral.

Let us see how the external electric field gives the electric current in this system. We are interested in a homogeneous configuration in the 3-dimensional space in the gauge theory side, and thus, we simply put $\partial_x = 0$. Then the equations of motion are

$$\begin{aligned} \partial_z \left[\frac{F_{0z}}{z\sqrt{\xi}} \right] &= 0, & \partial_0 \left[\frac{F_{0z}}{z\sqrt{\xi}} \right] &= 0, \\ \partial_z \left[\left(1 - \frac{z^4}{z_H^4}\right) \frac{F_{1z}}{z\sqrt{\xi}} \right] &+ \partial_0 \left[\left(1 - \frac{z^4}{z_H^4}\right)^{-1} \frac{F_{01}}{z\sqrt{\xi}} \right] &= 0. \end{aligned} \quad (2.6)$$

⁵The fluctuation modes of the gauge fields on the D7-branes correspond to meson modes in the gauge theory side.

In particular when the field configuration is time-independent, we put $\partial_0 = 0$ and obtain

$$\partial_z \left[\frac{F_{1z}}{z\sqrt{\xi}} \left(1 - \frac{z^4}{z_H^4} \right) \right] = 0, \quad \partial_z \left(\frac{F_{0z}}{z\sqrt{\xi}} \right) = 0. \quad (2.7)$$

Note that a configuration of a constant field strength, $F_{01} = \text{constant}$, with $F_{1z} = F_{0z} = 0$, solves the equations of motion.

One can obtain a generic nontrivial solution, since from the equations (2.7), two integration constants j and d can be found,

$$j = \frac{2\pi\alpha' F_{1z}}{z\sqrt{\xi}} \left(1 - \frac{z^4}{z_H^4} \right), \quad d = \frac{2\pi\alpha' F_{0z}}{z\sqrt{\xi}}. \quad (2.8)$$

Up to some normalization, j is the electric current, and d is the charge density. The solution can be explicitly written as

$$A_0 = \mu - \int_0^z dz \frac{d}{2\pi\alpha'} z\sqrt{\xi}, \quad (2.9)$$

$$A_1 = Et - \int_0^z dz \frac{j}{2\pi\alpha'} z\sqrt{\xi} \left(1 - \frac{z^4}{z_H^4} \right)^{-1}, \quad (2.10)$$

$$A_z = 0. \quad (2.11)$$

Here, $E = F_{01}$ is a constant electric field. In these expressions, ξ is given by

$$\xi = \frac{1 - \frac{(2\pi\alpha')^2 z^4}{R^4} E^2 \left(1 - \frac{z^4}{z_H^4} \right)^{-1}}{1 + \frac{z^6}{R^4} \left\{ d^2 - j^2 \left(1 - \frac{z^4}{z_H^4} \right)^{-1} \right\}}. \quad (2.12)$$

This was obtained by substituting (2.8) into the original definition of ξ (2.5) and solve it for ξ .

It seems that j can be determined irrespective of the electric field E , but it is not the case. Interestingly, the relation between E and j comes from the reality condition of the D-brane action [47, 52, 53].⁶ Stable configuration of D-branes should not admit an imaginary part of the action. However, in generic choice of E , j and d , the quantity ξ given by (2.12) can be negative, and since the action has a factor $\sqrt{\xi}$, it leads to an imaginary part. So, any stable configuration demands that ξ should not be negative. This means that at a certain z the denominator changes its sign and at the same z the numerator should change its sign. Denoting this position z as z_p , z_p should solve two equations

$$1 + \frac{z_p^6}{R^4} \left\{ d^2 - j^2 \left(1 - \frac{z_p^4}{z_H^4} \right)^{-1} \right\} = 0, \quad (2.13)$$

$$1 - \frac{(2\pi\alpha')^2 z_p^4}{R^4} F_{01}^2 \left(1 - \frac{z_p^4}{z_H^4} \right)^{-1} = 0. \quad (2.14)$$

⁶The reality condition is reminiscent of that for a fundamental string in the AdS_5 black hole, for computing a quark drag force [54, 55].

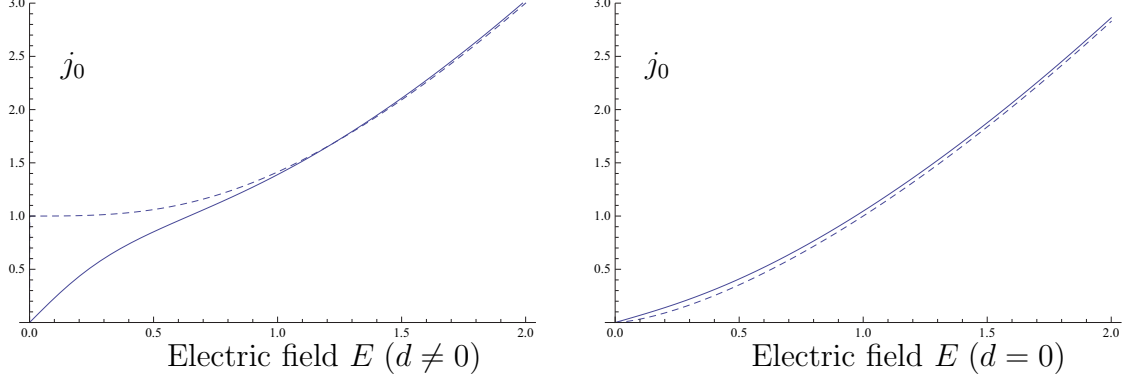


Figure 4: IV -characteristics of our massless supersymmetric QCD, given by eqn.(2.15). The left (right) corresponds to a doped $d = 1$ (non-doped $d = 0$) system. The dashed lines are for zero temperature $z_H = \infty$, while the solid lines are at a finite temperature $z_H = 1.5$. We have set $R = 1$ and $2\pi\alpha' = 1$.

Eliminating z_p , we obtain the stable current $j = j_0$ written in terms of the electric field E , the charge density d and the temperature T as

$$j_0 = \sqrt{d^2 + \frac{((2\pi\alpha'E)^2 + R^4/z_H^4)^{3/2}}{R^2}} \frac{2\pi\alpha'E}{\sqrt{(2\pi\alpha'E)^2 + R^4/z_H^4}}. \quad (2.15)$$

This is the I - V curve of our massless supersymmetric QCD which is shown in Fig. 4.

As a reference, we summarize two limits for this expression. When the density is zero ($d = 0$), we have

$$j_0 = \frac{2\pi\alpha'E}{Rz_H} (R^4 + (2\pi\alpha'E)^2 z_H^4)^{1/4}. \quad (2.16)$$

When the temperature is zero ($z_H = \infty$), we have

$$j_0 = \sqrt{d^2 + \frac{(2\pi\alpha'E)^3}{R^2}}. \quad (2.17)$$

We shall argue the meaning of the I - V curve (2.15). In terms of the resistivity $\rho \equiv E/j_0$, our I - V curve (2.15) gives the following relation, at the linear response $E \sim 0$,

$$\rho \sim \frac{T^2}{\sqrt{d^2 + T^6}}. \quad (2.18)$$

Here in (2.18), to discuss a physical interpretation, we have ignored all numerical coefficients and the λ - and N_c - dependence. Let us see the temperature dependence for fixed $d \neq 0$ (doped). Our resistivity (2.18) shows an interesting behavior: At low temperature, it is a metal with a Fermi liquid like behavior ($\rho \sim T^2$), while at high temperature it exhibits an insulator-type resistivity $d\rho/dT < 0$. This is interesting in

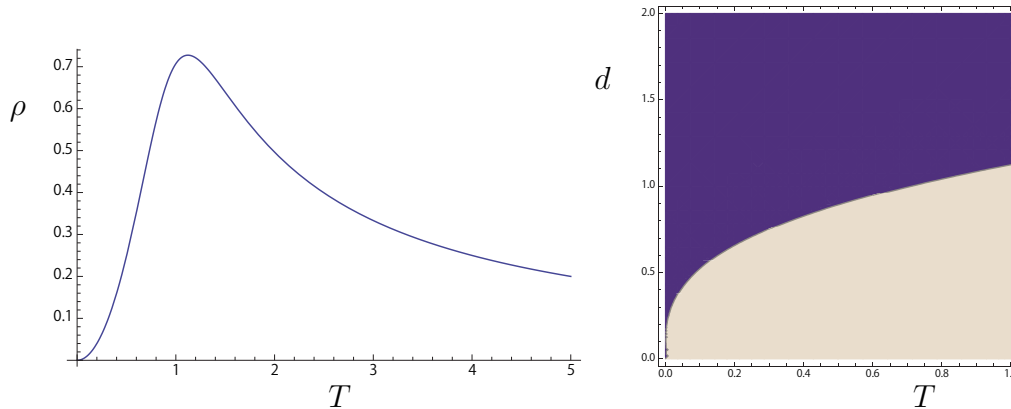


Figure 5: Left: The resistivity (2.18) at a finite charge density as a function of T . We have taken $d = 1$. Right: The plot of $d\rho/dT$, the dark region gives an insulator-like phase $d\rho/dT < 0$, while the light region is a metallic phase $d\rho/dT > 0$. At low temperature for fixed density d , we have Fermi-liquid like behavior $\rho \sim T^2$.

two viewpoints. First, in holographic setups obtaining a Fermi-liquid is non-trivial since the system is in the strongly interacting limit and the fermion propagators usually show abnormal behaviors. Second, in most materials, the high temperature side of the phase diagram shows metallic physics while non-Fermi liquid is found in the low temperature side. This is opposite to what we observe. One possible reason for this comes from the fact that our system is not a pure Fermion system but also consists of strongly coupled bosons; In the high temperature regime, the bosons become highly excited which may disturb the transport of the fermions. The case with zero doping $d = 0$ shows a very peculiar strange metal behavior with $\rho \sim 1/T$ [47].

In the section, we have reviewed the I - V curve of the $\mathcal{N} = 2$ supersymmetric QCD, at finite quark density. The reality condition imposed on the D-brane action determines the current j as a function of the electric field E .

3. Vacuum instability in a holographic gapless system

Let us consider a sudden application of an electric field to the system. Then it is expected that the system, which has been the vacuum, would become unstable. The instability is measured by the imaginary part of the effective action.

In the previous section, the I - V curve of the supersymmetric QCD was derived by imposing the reality condition of the D-brane action. In this section, we relax this condition and study the physical meaning of the imaginary part. We treat a gapless system (massless QCD) first, and in the next section we generalize our result to a gapped system (massive QCD).

The imaginary part in the D-brane effective Lagrangian signals some instability. In our case, it is natural to expect that the instability is related to the existence

of a more stable configuration; a phase with a constant electric current at which the effective Lagrangian is no more imaginary. In the past, the imaginary part of D-brane actions has not been a subject of intensive study. However, D-brane actions are nothing but an open string partition function (as seen from an off-shell formulation of string theory — boundary string field theory), and it has been discussed that open strings in a background electric field develops instability associated with tachyonic modes [56, 57, 24, 25]. Here our idea is to look into the imaginary part of the flavor D-brane action in the gauge/gravity duality, seriously.

3.1 The effective Lagrangian

When the electric field is suddenly turned on at $t = 0$, the original vacuum solution given by $j = 0$ becomes unstable in the presence of an electric field, and the reality condition which we considered in the previous section cannot be met. Let us investigate this simplest situation. Let us put $j = 0$ in the D7-brane effective Lagrangian ⁷

$$\mathcal{L} = -2\pi^2\mu_7 \int_0^{z_H} dz \frac{R^8}{z^5} \sqrt{\left[1 + \frac{z^6 d^2}{R^4}\right]^{-1} \left[1 - \frac{(2\pi\alpha')^2 z^4}{R^4} E^2 \left(1 - \frac{z^4}{z_H^4}\right)^{-1}\right]}. \quad (3.1)$$

From the square root in the expression, we notice that the integrand is real for small z , but at a certain z_* , it changes from a real function to an imaginary function:

$$z = z_* \equiv \alpha z_H, \quad \alpha \equiv \left(1 + \frac{(2\pi\alpha')^2 z_H^4}{R^4} E^2\right)^{-1/4}. \quad (3.2)$$

Since $z_* < z_H$ for nonzero E and nonzero z_H (the vanishing z_H means infinite temperature $T = \infty$), there always exists imaginary \mathcal{L} .

As briefly explained in the introduction, Fig. 2 illustrates the brane configuration and the regions of the brane which give the real and the imaginary parts of the D-brane action. The flat sheet denotes the D7-brane in the $AdS_5 \times S^5$ geometry. When there is no current, the central region of the D7-brane (indicated by the inside of a sphere whose radius is z_*), given by $z > z_*$, contributes to the imaginary part. The outer region, closer to the boundary of the AdS_5 , contributes to the real part of the D7-brane effective Lagrangian through the integration. On the other hand, when there exists the current, we can make all the region to be giving a real number for the D7-brane action, as we have reviewed in the previous section.

⁷The terminology ‘‘Lagrangian’’ is used since this function describes the dynamics of the electromagnetic field which is coupled to the QCD degrees of freedom. The QCD degrees of freedom is integrated away and is effectively described by the (log of the) partition function calculated via holography, which is represented as a z integral.

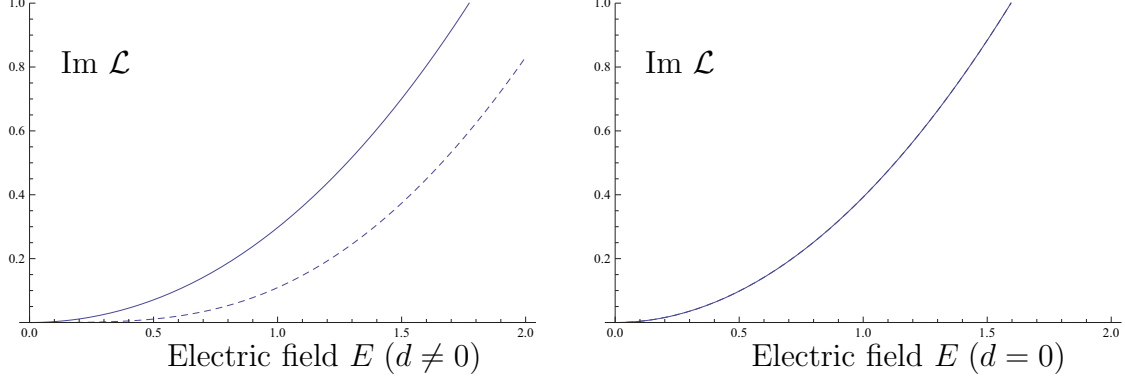


Figure 6: The imaginary part of the lagrangian of our massless supersymmetric QCD, given by (3.5). The left (right) corresponds to a doped $d = 1$ (non-doped $d = 0$) system. The dashed lines are for zero temperature $z_H = \infty$, while the solid lines are at a finite temperature $z_H = 1$. We have set $R = 1$ and $2\pi\alpha' = 1$. For no doping ($d = 0$), there is no temperature dependence.

In terms of z_* , the effective Lagrangian (3.1) simplifies to the following expression,

$$\mathcal{L} = -2\pi^2\mu_7R^6\sqrt{R^4 + (2\pi\alpha')^2E^2z_H^4}\int_0^{z_H} dz \frac{1}{z^5}\sqrt{\frac{z_*^4 - z^4}{(1 + d^2z^6/R^6)(z_H^4 - z^4)}}. \quad (3.3)$$

Defining $y \equiv z/z_H$, we obtain explicit integral formulas for the real and the imaginary parts of the effective Lagrangian,

$$\text{Re}\mathcal{L} = -2\pi^2\mu_7\frac{R^8}{z_H^4\alpha^2}\int_0^\alpha dy \frac{1}{y^5}\sqrt{\frac{\alpha^4 - y^4}{(1 + d^2z_H^6y^6/R^6)(1 - y^4)}}, \quad (3.4)$$

$$\text{Im}\mathcal{L} = 2\pi^2\mu_7\frac{R^8}{z_H^4\alpha^2}\int_\alpha^1 dy \frac{1}{y^5}\sqrt{\frac{y^4 - \alpha^4}{(1 + d^2z_H^6y^6/R^6)(1 - y^4)}}. \quad (3.5)$$

Here, the electric field dependence is included in α , and the temperature in z_H . The imaginary part (3.5)⁸ characterizes the vacuum instability of the $\mathcal{N} = 2$ supersymmetric QCD, at the large N_c and at the strong coupling limit.

Fig. 6 is a plot of the imaginary part of the effective Lagrangian (3.5) as a function of E . Obviously, it is a monotonic function of E , and it agrees with the intuition that larger values of E would induce stronger instability. The plot also shows that in doped ($d \neq 0$) systems the imaginary part increases as the temperature increases. This again is consistent with the intuition that there are more decay channels in systems with higher temperature to the current flowing state. The zero-temperature case is analyzed in App.A.

⁸The sign of the imaginary part is chosen to be positive among $-1 = (\pm i)^2$.

3.2 Coincidence with Schwinger at vanishing density

The imaginary part of the effective Lagrangian (3.5) is a function of the electric field E , the temperature T and the charge density d . Let us consider the case of no doping, $d = 0$. Using the formula

$$\int_{\alpha}^1 dy \frac{1}{y^5} \sqrt{\frac{y^4 - \alpha^4}{1 - y^4}} = \frac{\pi}{8} \frac{1 - \alpha^4}{\alpha^2}, \quad (3.6)$$

the imaginary part (3.5) is rewritten as

$$\text{Im } \mathcal{L} \Big|_{d=0} = \frac{\pi^3}{4} \mu_7 R^4 (2\pi\alpha')^2 E^2. \quad (3.7)$$

We use the string theory expressions for the AdS radius R and the D7-brane tension μ_7 as

$$R^4 = (2\pi\alpha')^2 \frac{\lambda}{2\pi^2}, \quad \mu_7 = \frac{1}{(2\pi)^7 g_s \alpha'^4} = \frac{1}{4\pi^2 g_{\text{S}^2}^2 (2\pi\alpha')^4}, \quad (3.8)$$

then the imaginary part (3.5) is written solely by N_c and the electric field as

$$\text{Im } \mathcal{L} \Big|_{d=0} = \frac{N_c}{32\pi} E^2. \quad (3.9)$$

Quite surprisingly, our result (3.9) coincides with the standard result for the QED vacuum instability by Schwinger [19] and Weisskopf [18] discussed in the introduction, *i.e.*, eqns. (1.6) and (1.7)⁹. To compare them with our result, we take a massless limit $m = 0$, and use formulas $\sum_{n=1}^{\infty} n^{-2} = \pi^2/6$, $\sum_{n=1}^{\infty} (-1)^{n-1} n^{-2} = \pi^2/12$. Furthermore, since we are working in the $\mathcal{N} = 2$ supersymmetric QCD, the charged matter fields consist of an $\mathcal{N} = 2$ hypermultiplet (a single Dirac fermion and two complex scalars). It turns out that the total Schwinger effect is

$$N_c \left(\text{Im } \mathcal{L}_{\text{spinor}}^{1\text{-loop}} \Big|_{m_e=0} + 2 \text{Im } \mathcal{L}_{\text{scalar}}^{1\text{-loop}} \Big|_{m_e=0} \right) = \frac{N_c}{32\pi} E^2. \quad (3.10)$$

The factor N_c is from the number of hypermultiplets (as they are in the fundamental representation of $SU(N_c)$ color symmetry). This one loop QED result of the Schwinger effect (3.10) agrees with our imaginary part (3.9).

This agreement is somewhat unexpected: In our $\mathcal{N} = 2$ supersymmetric QCD we are working in the strong coupling limit where the effective action should include information of all the summation of the gluon-exchange diagrams, while the calculation of the one loop Euler-Heisenberg effective Lagrangian in QED (and the scalar QED) is done in the free limit with no photon nor gluon mediated interactions. In

⁹Note that in the standard normalization of gauge fields our E is written as eE where e is the gauge coupling constant.

addition, we have no supersymmetry once we turned on the electric field, so, BPS properties which may often protect observables from perturbative gluonic corrections are not expected. In the next section, we generalize our calculation to the massive case, and will see further agreement.

We have one more comment on our result (3.9), which is the independence from the temperature. Although we are working with arbitrary temperature, the result (3.9) does not depend on the temperature. This is natural from the Schwinger mechanism viewpoint, as follows. First, the instanton action of the electron in the background electric field is made by a circular worldline of the electron in Euclideanized spacetime whose radius is m/E , and the effect of the temperature appears in the periodicity in the Euclideanized time direction. So if $2\pi/T > m/E$, the temperature should give no effect on the instanton action. Because we took the gapless limit $m = 0$, this inequality is always satisfied, so there should be no temperature-dependence in the Schwinger's result. Our temperature independence in (3.9) indicates that this intuitive picture via instantons may hold even at our strong coupling limit for gluons.

3.3 Energy difference between the $j = 0$ and $j = j_0$ states

Let us look more closely at the real part of the Euler-Heisenberg Lagrangian (3.4). When the background temperature is zero ($z_H = \infty$), the expression simplifies to

$$\text{Re } \mathcal{L}_{\text{unstable}} = -2\pi^2 \mu_7 \frac{(2\pi\alpha'E)^2 R^4}{2} \int_0^1 \frac{d\tilde{y}}{\tilde{y}^3} \sqrt{1 - \tilde{y}^2}, \quad (3.11)$$

where we have shifted the integration variable as $\tilde{y} \equiv \alpha y$. This corresponds to the energy of the total unstable system.

Now, suppose the system relaxes to another phase where we have a constant electric current. This state is reviewed in section 2, and we expect that our instability shown by the imaginary part signals the decay to this state with the current. So, let us look at the energy difference between our unstable system given by (3.11) and the energy of the stable state with the current.

When we have the electric current, the D-brane effective action is given by $\sim \sqrt{\xi}$ where ξ is given by (2.12). The effective Lagrangian is easily evaluated, with $d = 0$ and $j_0 \neq 0$, with the integration variable and boundary chosen in such a way that the Lagrangian is real,

$$\text{Re } \mathcal{L}_{\text{stable}} = -2\pi^2 \mu_7 \frac{(2\pi\alpha'E)^2 R^4}{2} \int_0^1 \frac{d\tilde{y}}{\tilde{y}^3} \sqrt{\frac{1 - \tilde{y}^2}{1 - \tilde{y}^3}}. \quad (3.12)$$

We are interested in the energy difference, and it can be calculated as

$$\text{Re } \mathcal{L}_{\text{unstable}} - \text{Re } \mathcal{L}_{\text{stable}} = \frac{c}{8\pi^2} N_c E^2, \quad (3.13)$$

with a positive numerical constant $c \sim 0.855$. It is quite intriguing that the energy difference is actually finite, and the real part of our complex effective Lagrangian certainly makes sense.¹⁰

4. Vacuum instability in holographic system with mass gap

A more interesting setup is a strongly correlated system with a mass gap. In this section, we consider the case with massive quarks. In the $\mathcal{N} = 2$ supersymmetric QCD, we can turn on the mass for the hypermultiplet. The quark and the squark have the same mass m_q . In the holographic description, this quark mass is translated to the distance between the D7-brane and the N_c D3-branes.

We work out the real part and the imaginary part of the D7-brane effective action in the $AdS_5 \times S^5$ spacetime, to obtain the full Euler-Heisenberg Lagrangian. We find that the imaginary part develops only for E larger than the critical electric field E_{cr} set by the confining potential. This is what we expect from the example of $1 + 1$ dimensional QED, the massive Schwinger model. We shall also see that the first two terms in the large E expansion of the imaginary part of the Lagrangian coincides with the weak coupling Schwinger calculation, somehow unexpectedly.

4.1 Critical electric field and the confining force

Our goal here is to write down the D7-brane action with finite external electric fields for a massive system. The massive version of our D3/D7 system is described by a geometry where the D7-brane is separated from the center of the AdS_5 geometry. In the absence of the electric field, the D7-brane is just a flat hyperplane [23]. So, we consider a flat D7-brane in the AdS_5 , and put a constant electric field E on the D7-brane.¹¹

Let us consider the quark mass m_q . The distance between the D7-brane and the center of AdS_5 is given by $\eta = 2\pi\alpha' m_q$, as the fundamental string tension is

¹⁰Readers may have suspected that there would be a divergence in energy formulas. In fact there appears a divergence but it can be removed by a holographic renormalization [58, 59]. Here we are evaluating the difference, so there is no need to perform explicitly the holographic renormalization.

¹¹Note that when the electric field is turned on in the massive case, in order to analyze the D-brane time evolution, the bending of the D7 brane described by the scalar field must be taken into account. This is in contrast to the massless case where the flat D7-brane solves the equations of motion. However, this difficulty does not appear in the calculation of the vacuum instability described by the effective Lagrangian: We only need the zero field solution, and not the full time dependent solution. This is because we are not interested in the final stable configuration but only in the instability of the initial vacuum state. The Euler-Heisenberg Lagrangian captures the instability as well as the nonlinear properties of the vacuum. It is related to the vacuum persistence amplitude by $\langle 0|U(t)|0\rangle = e^{i\mathcal{L}vt}$ (v : spatial volume), where $|0\rangle$ is the vacuum without the electric field while $U(t)$ is the time-evolution matrix with the electric field. The on-shell time evolution will be studied in section 5.

given by $\mathcal{T}_{F1} = 1/(2\pi\alpha')$. At zero temperature, the background is just the $AdS_5 \times S^5$ geometry, and the D7-brane action with the constant electric field $F_{0x} = E$ is given by

$$\mathcal{L} = -2\pi^2\mu_7 \int_0^\infty dz \frac{R^8}{z^5} \sqrt{1 - \frac{(2\pi\alpha')^2 R^4}{(\eta^2 + R^2/z^2)} E^2}. \quad (4.1)$$

Obviously, putting $\eta = 0$ brings it back to the previous case (2.4). z is the radial coordinate, and $z = \infty$ is the boundary.

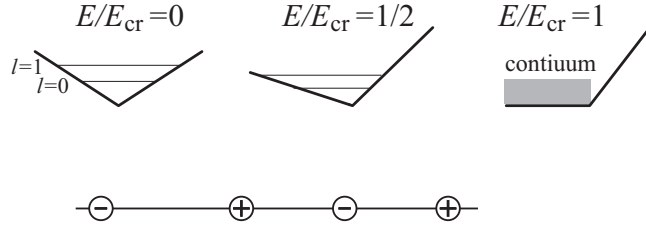


Figure 7: Above: Schematic confining potential of the quark and antiquark in the presence of an electric field. At $E = E_{cr}$, the potential becomes flat in one direction inducing the liberation of the quark-antiquark pair. This leads an emergent massless continuum states. Below: Coleman's half-asymptotic state realized at $E = E_{cr}$ in the massive Schwinger model. Quarks and antiquarks can freely move in the direction of the electric field as long as the charges are in a plus-minus-plus-... order.

Now, as before, the factor inside the square root can be negative, which gives us the imaginary part of the action. The square root becomes zero at

$$z = z_0 \equiv \frac{R^2}{\sqrt{2\pi\alpha' R^2 E - \eta^2}}. \quad (4.2)$$

So, if this z_0 exists, we have the imaginary action. The condition for existence of the imaginary part is

$$E > E_{cr} \equiv \frac{\eta^2}{2\pi\alpha' R^2} = \frac{\sqrt{2}\pi}{\sqrt{\lambda}} m_q^2. \quad (4.3)$$

We find that there is a critical electric field beyond which the action develops an imaginary value.

Now, the important lesson from the massive Schwinger model (1+1-dimensional QED with massive electrons) [22] is that the originally confined charges become liberated when the external electric field acting on the electron positron pair balances the confining force between them (see Fig. 7). So let us compare the critical electric field (4.3) obtained from the D7-brane action and see whether it coincide with the confining force. In Ref. [60], from the computation of small Wilson loop on the D7-brane, the QCD string tension at the meson sector of the D3D7 model was calculated.

The quark antiquark potential for distance L is given by

$$V = \frac{\sqrt{2\pi}}{\sqrt{\lambda}} m^2 L. \quad (4.4)$$

Comparing it with (4.3), the confining force exactly agrees with our critical electric field.

We confirmed the physical intuition that the instability of the system becomes present only when we have an electric field large enough to cancel the confining force. This indicates that generically systems with confining force may have a similar behavior.

4.2 Imaginary part: coincidence with Schwinger

Let us examine the imaginary part of the D7-brane action (4.1). The imaginary part comes from the integral over the region $z_0 < z < \infty$,

$$\text{Im } \mathcal{L} = 2\pi^2 \mu_7 (2\pi\alpha') R^{10} \sqrt{E^2 - E_{\text{cr}}^2} \int_{z_0}^{\infty} dz \frac{\sqrt{(z^2 - z_0^2)(z^2 + \tilde{z}_0^2)}}{z^5 (z^2 \eta^2 + R^4)}, \quad (4.5)$$

where we have defined

$$\tilde{z}_0 \equiv \frac{R^2}{\sqrt{2\pi\alpha' R^2 E + \eta^2}}. \quad (4.6)$$

In Fig. 8, this imaginary part (4.5) is shown. A smooth increase of the imaginary part, starting at $E = E_{\text{cr}}$, is observed.

We want to compare our result with the QED results, *i.e.*, (1.6) and (1.7). In the massless QCD case studied in the previous section, we saw complete agreement of the imaginary part of the effective Lagrangian. In the present massive case, since we have another mass scale, which is the quark mass, it is appropriate to consider the large E expansion. The reason is that at small E , because of the confinement taking place below the energy scale $m^2/\sqrt{\lambda}$ in QCD, there should be no agreement between QED.

To investigate the large E behavior, let us define $\epsilon \equiv E_{\text{cr}}/E$ and use a new radial coordinate

$$v \equiv \frac{z^2}{z_0^2} - 1. \quad (4.7)$$

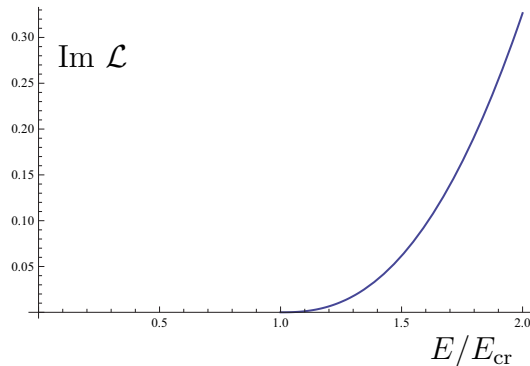


Figure 8: The imaginary part of the Lagrangian of our massive supersymmetric QCD, given by (4.8).

Then the imaginary part (4.5) is rewritten as

$$\begin{aligned}\text{Im}\mathcal{L} &= \pi^2 \mu_7 (2\pi\alpha')^2 R^4 E_{\text{cr}}^2 \frac{(1-\epsilon)^{5/2}}{\epsilon^2} \int_0^\infty dv \frac{\sqrt{v(2+v+\epsilon v)}}{(v+1)^3(1+\epsilon v)} \\ &= \frac{N_c}{8\pi^2} E_{\text{cr}}^2 \frac{(1-\epsilon)^{5/2}}{\epsilon^2} \int_0^\infty dv \frac{\sqrt{v(2+v+\epsilon v)}}{(v+1)^3(1+\epsilon v)}.\end{aligned}\quad (4.8)$$

Let us expand this D-brane result for a large E , *i.e.* the small ϵ expansion,

$$\frac{(1-\epsilon)^{5/2}}{\epsilon^2} \int_0^\infty dv \frac{\sqrt{v(2+v+\epsilon v)}}{(v+1)^3(1+\epsilon v)} = \frac{\pi}{4} \frac{1}{\epsilon^2} \left(1 + \frac{4}{\pi} \epsilon \log \frac{\epsilon}{2} - \frac{1}{3\pi} \epsilon^3 + \mathcal{O}(\epsilon^4) \right). \quad (4.9)$$

In terms of the physical quantities, this is equivalent to the following expression of the imaginary part,

$$\text{Im}\mathcal{L} = \frac{N_c}{32\pi} E^2 \left(1 + \frac{4}{\pi} \frac{E_{\text{cr}}}{E} \log \frac{E_{\text{cr}}}{2E} - \frac{1}{3\pi} \left(\frac{E_{\text{cr}}}{E} \right)^3 + \mathcal{O} \left(\left(\frac{E_{\text{cr}}}{E} \right)^4 \right) \right). \quad (4.10)$$

Of course for a massless quark limit $m = 0$, in other words $E_{\text{cr}} = 0$, this expression reduces to the massless QCD case (3.9). Because of the nonzero mass m , we find a sub-leading correction of the form $(E_{\text{cr}}/E) \log(E_{\text{cr}}/E)$.

Although there is no strong reason for us to expect that this supersymmetric QCD result should agree with the Schwinger's QED result, let us anyway compare them. The QCD result is (1.6) and (1.7), which is in fact a sum of dilogarithmic functions,

$$\begin{aligned}N_c \left(\text{Im} \mathcal{L}_{\text{spinor}}^{1\text{-loop}} + 2 \text{Im} \mathcal{L}_{\text{scalar}}^{1\text{-loop}} \right) \\ = \frac{N_c}{8\pi^3} E^2 \left[\text{Li}_2(\exp(-m_e^2 \pi/E)) - \text{Li}_2(-\exp(-m_e^2 \pi/E)) \right].\end{aligned}\quad (4.11)$$

where $\text{Li}_2(z) \equiv \sum_{n=1}^\infty z^n/n^2$ is the dilogarithm function. Using the known expansion of the dilogarithm functions, we obtain

$$\text{Im} \mathcal{L}_{N_c \text{spinor} + 2N_c \text{scalar}}^{1\text{-loop}} = \frac{N_c}{32\pi} E^2 \left(1 + \frac{4}{\pi} \frac{m_e^2}{E} \log \frac{m_e^2 \pi}{2eE} - \frac{1}{9\pi^2} \left(\frac{m_e^2 \pi}{E} \right)^3 + \mathcal{O} \left(\left(\frac{m_e^2 \pi}{E} \right)^4 \right) \right). \quad (4.12)$$

Note here that e in this expression is the base of natural logarithms, not the electric charge. We notice that at the nontrivial sub-leading order, this expression coincides with the supersymmetric QCD at strong coupling, (4.10), once we identify

$$E_{\text{cr}} \leftrightarrow m_e^2. \quad (4.13)$$

This coincidence is quite nontrivial. First, in the holographic QCD calculation, we have infinite gluon exchanges while in QED of course there is no gluon. Second,

although the QCD side has supersymmetries, the electric field breaks the supersymmetries completely, so we cannot generically expect any cancellation of the higher diagrams via the supersymmetries. Nevertheless we obtained interesting coincidence between the famous 1-loop QED results with our holographic calculation of the imaginary part of the effective action. One possible reason for this is due to some conformal symmetry in the gluon sector, but we leave the detailed research for a future work.

4.3 Euler-Heisenberg Lagrangian

So far, we focused on the imaginary part of the effective action. In the present subsection we will examine the real part.

4.3.1 Effective action below the critical electric field

When $E \leq E_{\text{cr}}$, the D7-brane action, *i.e.*, the Euler-Heisenberg action, remains real. It is important to obtain the series expansion in E since the coefficients become the “non-linear optical response function”. Using the expansion formula

$$\sqrt{1-x} = 1 + \sum_{n=1}^{\infty} \frac{(2n-3)!!}{n!} \left(\frac{-x}{2}\right)^n, \quad (4.14)$$

we can evaluate the integral in (4.5) term by term after the expansion, to obtain

$$\begin{aligned} \mathcal{L} = & -2\pi^2 \mu_7 R^8 \left[\int_{\delta z}^{\infty} \frac{dz}{z^5} + \frac{(2\pi\alpha')^2}{4R^4} \left(1 + \log \frac{\eta^2(\delta z)^2}{R^4} \right) E^2 \right. \\ & \left. + \frac{\eta^4}{R^8} \sum_{n=2}^{\infty} \frac{(2n-3)!!}{4(2n-1)(n-1)n!} \left(\frac{-(2\pi\alpha')^2 R^4}{2\eta^4} \right)^n E^{2n} \right]. \quad (4.15) \end{aligned}$$

In this expression, The term E^{2n} with $n = 0$ and $n = 1$ has a divergent coefficient, so we included a UV cutoff $z = \delta z$, so that the integral is for the region $\delta z < z < \infty$. Following the standard holographic renormalization technique [58, 59], we add a local counter term,

$$\delta\mathcal{L} = 2\pi^2 \mu_7 R^8 \left[\int_{\delta z}^{\infty} \frac{dz}{z^5} + \frac{(2\pi\alpha')^2 E^2}{4R^4} \log \frac{\eta^2(\delta z)^2}{R^4} \right] \quad (4.16)$$

The coefficients (the finite term) are determined in such a way that the renormalized action does not have any α' dependence if written in terms of the gauge theory variables. After the subtraction, we finally arrive at the expression for the Euler-Heisenberg Lagrangian,

$$\mathcal{L} = -\frac{N_c}{16\pi^2} E^2 - \frac{N_c \lambda}{8\pi^4} E_{\text{cr}}^2 \sum_{n=2}^{\infty} \frac{(2n-3)!!}{4(2n-1)(n-1)n!} \left(\frac{-E^2}{2E_{\text{cr}}^2} \right)^n. \quad (4.17)$$

We have found an infinite tower of nonlinear responses in the electric field. Note that the coefficient of the first term, which is a charge renormalization, has ambiguity as a renormalization scheme dependence.

4.3.2 Effective action above the critical electric field

When the electric field exceeds the critical field $E > E_{\text{cr}}$, the integral region that contributes to the real part of the effective action is restricted to $0 < z < z_0$. The integral becomes

$$\text{Re } \mathcal{L} = -2\pi^2 \mu_7 (2\pi\alpha') R^{10} \sqrt{E^2 - E_{\text{cr}}^2} \int_0^{z_0} dz \frac{\sqrt{(z_0^2 - z^2)(z^2 + \tilde{z}_0^2)}}{z^5 (z^2 \eta^2 + R^4)}. \quad (4.18)$$

Using a new coordinate $u \equiv z^2/z_0^2$, we obtain

$$\text{Re } \mathcal{L} = -\pi^2 \mu_7 (2\pi\alpha')^2 R^4 E_{\text{cr}}^2 \frac{(1 - \epsilon^2)^{5/2}}{\epsilon^2} \int_0^1 \frac{du}{u^3} \frac{\sqrt{(1-u)(u+1+\epsilon(u-1))}}{1+\epsilon(u-1)}. \quad (4.19)$$

The integral is divergent, but with a UV cutoff $u = \delta$ it can be exactly calculated as

$$\begin{aligned} & \frac{(1 - \epsilon^2)^{5/2}}{\epsilon^2} \int_{\delta}^1 \frac{du}{u^3} \frac{\sqrt{(1-u)(u+1+\epsilon(u-1))}}{1+\epsilon(u-1)} \\ &= \frac{-(3 + \log 2)}{2} \epsilon^{-2} + \frac{-\pi}{2} \epsilon^{-1} - \frac{1}{2} - \frac{1}{2} \epsilon^{-2} \log \epsilon + I_{\text{div}} \end{aligned} \quad (4.20)$$

where

$$I_{\text{div}} \equiv \frac{1}{2} \left((\delta z)^2 \frac{\eta^2}{R^4} \right)^{-2} + \frac{1}{2\epsilon^2} \log \left[(\delta z)^2 \frac{\eta^2}{R^4} \right]. \quad (4.21)$$

Here we have used the relation between the cutoff in u and the cutoff in z ,

$$\delta = \frac{(\delta z)^2}{z_0^2} = (\delta z)^2 \frac{\eta^2}{R^4} \frac{1 - \epsilon}{\epsilon}. \quad (4.22)$$

This I_{div} is subtracted from the full effective action, by following the holographic renormalization (it is the same counter term as before.)

Finally, we obtain a finite real part of the Euler-Heisenberg Lagrangian,

$$\text{Re } \mathcal{L} = \frac{N_c}{8\pi^2} \left[\frac{3 + \log 2}{2} E^2 + \frac{\pi}{2} E_{\text{cr}} E + \frac{1}{2} E_{\text{cr}}^2 + \frac{1}{2} E^2 \log \frac{E_{\text{cr}}}{E} \right]. \quad (4.23)$$

Note that again the coefficient in front of the E^2 term has an ambiguity coming from the renormalization scheme dependence. The obtained Lagrangian has an interesting terms: the linear term E , and the log term $E^2 \log E$. We do not understand the reason that the effective Lagrangian suddenly acquires a term that is of odd power in the electric fields. It is expected to be related to the nature of the quantum state that appears at the critical field strength, with possible common aspects as Coleman's half asymptotic state [22].

5. Time-dependent process: relaxation and thermalization

Up to now, we have concentrated on the steady (un)stable state. One virtue of the gauge/gravity duality is that we can investigate time-dependent nonlinear responses of the system. In this section, we perform a time-dependent calculation of the system in which the electric field is switched on from zero to nonzero.

We expect two phenomena accordingly. One is the excitation and relaxation of the system, and the other is thermalization. Both are quite interesting and nontrivial in strongly correlated systems and are related to the physics studied experimentally at RHIC and LHC. Indeed we shall see in the following that the system relaxes to a nonequilibrium steady state with a constant current flow which is “thermalized”. The nonequilibrium thermal state is characterized by the *effective Hawking temperature* T_{eff} that we define below. This is calculated from the induced metric which depends on the D7-brane dynamics and thus on the external electric field. The effective Hawking temperature relaxes to a steady state value, which is nothing but the standard Hawking temperature for a given metric with a horizon, and through the gauge/gravity duality it is interpreted as a Matsubara temperature of the gauge theory.¹²

We find a universal behavior in this relaxation process. In fact, the time scale for the relaxation becomes universal, *i.e.*, no matter how quickly we apply the constant electric field, the thermalization time takes a value given by the Planckian time scale $1/T_{\text{eff}}$ with a parameter independent proportionality factor.

In this section, we first explain the calculation scheme in holography and then present results of the thermalization. We consider the massless case $\eta = 0$ throughout this section.

5.1 Equations of motion and effective Hawking temperature

The equations of motion for the massless case at zero temperature is (2.6) with $z_{\text{H}} = \infty$. We choose a gauge $A_z = 0$, then the equations of motion can be rewritten as follows:

$$\partial_z \left(\frac{F_{0z}}{z\sqrt{\xi}} \right) = 0, \quad \partial_0 \left(\frac{F_{0z}}{z\sqrt{\xi}} \right) = 0, \quad -\partial_z \left(\frac{\partial_z A_1}{z\sqrt{\xi}} \right) + \partial_0 \left(\frac{\partial_0 A_1}{z\sqrt{\xi}} \right) = 0. \quad (5.1)$$

From the first two equations, we can set

$$\frac{F_{0z}}{z\sqrt{\xi}} = d \quad (5.2)$$

¹²Note that our effective temperature is the temperature felt by fluctuation modes (mesons) on the D7-brane, and is different from the temperature of the background bulk geometry (the heat bath of gluons). In this section we set the bulk gluon temperature $T = 0$ (which corresponds to $z_{\text{H}} = \infty$ and the geometry is just the $AdS_5 \times S^5$).

using a constant d , which is nothing but the charge density, as we explained in section 2. Since $\xi = 1 - (z^4/R^4)\{(\partial_z A_0)^2 + (\partial_0 A_1)^2 - (\partial_z A_1)^2\}$, we have

$$\xi = \frac{1 - \frac{z^4}{R^4}\{(\partial_0 A_1)^2 - (\partial_z A_1)^2\}}{1 + \frac{z^6}{R^4}d^2}. \quad (5.3)$$

Thus, the explicit equations of motion for the gauge field A_1 is given by

$$-\partial_z \left(\frac{\sqrt{1 + \frac{z^6}{R^4}d^2}\partial_z A_1}{z\sqrt{1 - \frac{z^4}{R^4}\{(\partial_0 A_1)^2 - (\partial_z A_1)^2\}}} \right) + \partial_0 \left(\frac{\sqrt{1 + \frac{z^6}{R^4}d^2}\partial_0 A_1}{z\sqrt{1 - \frac{z^4}{R^4}\{(\partial_0 A_1)^2 - (\partial_z A_1)^2\}}} \right) = 0. \quad (5.4)$$

We can divide A_1 into two parts,

$$A_x = - \int^t E(s)ds + h(t, z), \quad (5.5)$$

where $E(t)$ is the external electric field, while $h(t, z)$ is a dynamical degree of freedom that satisfies $h(t, z=0) = 0$, $\partial_z h(t, z=0) = 0$. According to the standard AdS/CFT dictionary, the higher derivative term corresponds to the current j . To be precise, h is related to the current [47] by

$$\partial_z^2 h(t, z=0) = \langle J^x \rangle / \mathcal{N}, \quad (5.6)$$

where \mathcal{N} is a normalization factor.

Let us define an effective temperature for mesons. In any nonequilibrium time-dependent process, definition of the temperature is ambiguous. However, in the gravity dual part of the gauge/gravity duality, it is natural to define the temperature as an ‘‘effective Hawking temperature’’ defined from the inverse of the apparent horizon radius,

$$T_{\text{eff}} = \sqrt{\frac{3}{8}} \frac{1}{\pi z_{\text{AH}}}. \quad (5.7)$$

The apparent horizon converges to the event horizon once the system converges to a steady state, and in that asymptotic limit the above definition coincides with the standard Hawking temperature of a ‘‘black hole’’ made by the induced metric on the probe D7-brane. For the derivation of (5.7), see Appendix B.

The location of the apparent horizon $z = z_{\text{AH}}$ is defined as a time-dependent quantity. We follow the standard definition of the apparent horizon; it is defined as a hyper surface whose volume does not change if shifted along a null outward geodesics. First, using the induced metric of the gauge fields on the D7-branes, the

volume V_{AH} of a hypersphere with a fixed t and a fixed radius z becomes

$$\begin{aligned}
V_{\text{AH}} &= \int d^3 d^3 \theta^I \sqrt{G_{11} G_{22} G_{33} G_{I=1, I=1} G_{I=2, I=2} G_{I=3, I=3}} \\
&= V_3 \cdot \text{Vol}(S^3) \frac{R^6}{z^3} \mu_7^{-\frac{3}{2}} \left\{ 1 + \frac{z^4}{R^4} (2\pi\alpha')^2 (-F_{01}^2 - F_{0z}^2 + F_{1z}^2) \right\}^{3/4} \\
&\quad \times \left\{ 1 + \frac{z^4}{R^4} (2\pi\alpha')^2 (-F_{01}^2 + F_{1z}^2) \right\}^{1/2}. \quad (5.8)
\end{aligned}$$

Here G_{ab} is the effective metric which the gauge fluctuation on the D7-brane feels. The explicit expression is given in Appendix B. The null vector (v^t, v^z) in the (t, z) -slice satisfies

$$G_{ab} v^a v^b = 0. \quad (5.9)$$

The ratio of the components is calculated as

$$v_t/v_z = \frac{\frac{z^2}{R^2} 2\pi\alpha' F_{1z} \frac{z^2}{R^2} 2\pi\alpha' F_{01} + \sqrt{\xi}}{-1 + (\frac{z^2}{R^2} 2\pi\alpha' F_{01})^2}. \quad (5.10)$$

Using this, the position of the apparent horizon $z = z_{\text{AH}}(t)$ is defined by the solution of the equation

$$\delta V_{\text{AH}}(t, z_{\text{AH}}(t)) \equiv (v_t \partial_t + v_z \partial_z) V_{\text{AH}}(t, z) \Big|_{z=z_{\text{AH}}(t)} = 0. \quad (5.11)$$

The effective Hawking temperature $T_{\text{eff}}(t)$ defined by eqn. (5.7) is a function of the boundary time t . Suppose that the apparent horizon is at $(t_{\text{AH}}, z_{\text{AH}}(t_{\text{AH}}))$, then the boundary time t_b for this point is given by

$$t_b = t_{\text{AH}} + z_{\text{AH}}, \quad (5.12)$$

because the information of the presence of the apparent horizon of the brane needs to be propagated to the boundary via bulk geometry along the bulk null geodesics $(1, -1)$.

In the steady state limit ($t \rightarrow \infty$), the effective temperature should converge to the asymptotic value which is the Hawking temperature [61] given by

$$T_{\text{eff}}^\infty = \sqrt{\frac{3}{8}} \frac{1}{\pi z_p}. \quad (5.13)$$

This is because the apparent horizon approaches the event horizon given by $z = z_p$ on the D7-brane, c.f., (2.14), in the long time limit.

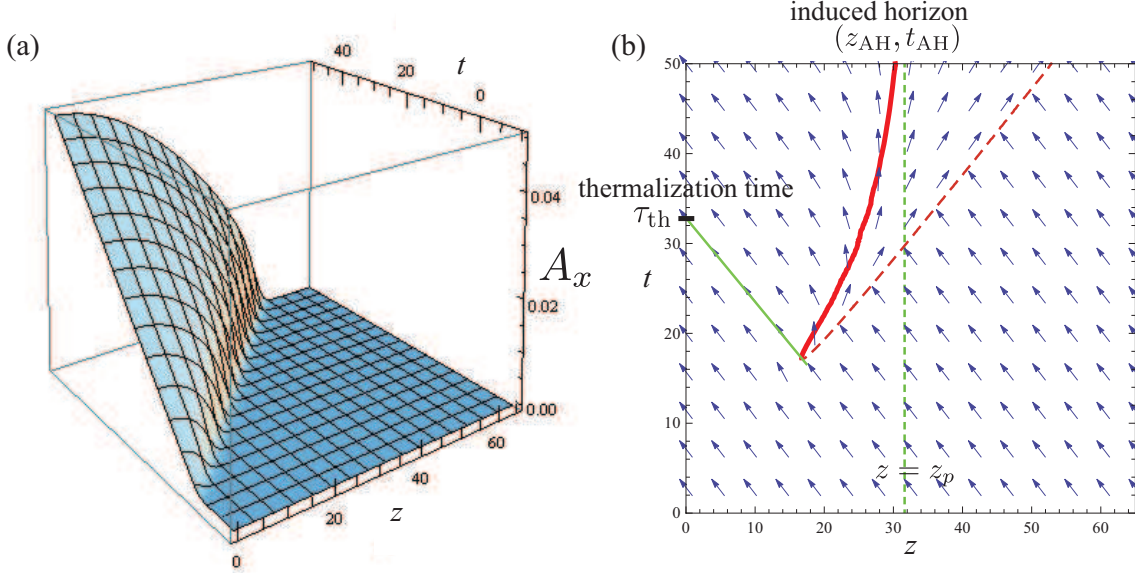


Figure 9: (a) The gauge field $A_x(z, t)$ for $E = 0.001$ in the undoped case ($d = 0$) calculated with parameters $T = 0$, $\omega = 0.7$, $R = 1$. (b) The induced horizon (red solid line). In the long time limit, it converges to the steady state value $z = z_p$ denoted by the green dotted line. The red (solid and dashed) lines are determined from the condition $\delta V_{\text{AH}} = 0$ given in (5.11). The vector field plots the direction of the null vector $(v_z, v_t)/\sqrt{v_z^2 + v_t^2}$.

5.2 Planckian thermalization accelerated by electric fields

We are ready to analyze explicitly the time-dependence of the system as a response to the change of the background electric field. At time $t = 0$, we smoothly switch on the electric field to its static value, given by (Fig. 10 (a))

$$E(t) = \frac{E}{2}(1 + \tanh(\omega t)). \quad (5.14)$$

The time length of the ramp is given by $1/\omega$. Here E is the constant electric field, so after a sufficient time, the system should relax to a nonequilibrium steady state with a constant current flow, which was reviewed in section 2. In numerical calculations, we use the normalization $2\pi\alpha' = 1$.

Figure 9 (a) plots the gauge field $A_1 = A_x(z, t)$ obtained by solving the equations of motion (5.4). After the electric field is switched on around $t = 0$, A_x begins to increase and this effect travels inward into the AdS direction. An apparent horizon is induced, which is determined by the condition (5.11); Two branches of solutions exist as plotted as the solid and dashed red lines in Fig. 9 (b). The apparent horizon corresponds to the branch that is closer to the boundary (solid line), which we denote by $(z_{\text{AH}}, t_{\text{AH}})$. This is confirmed by plotting the null vector direction (blue vector field) which points straight-upward (no z -component) on the horizon. The

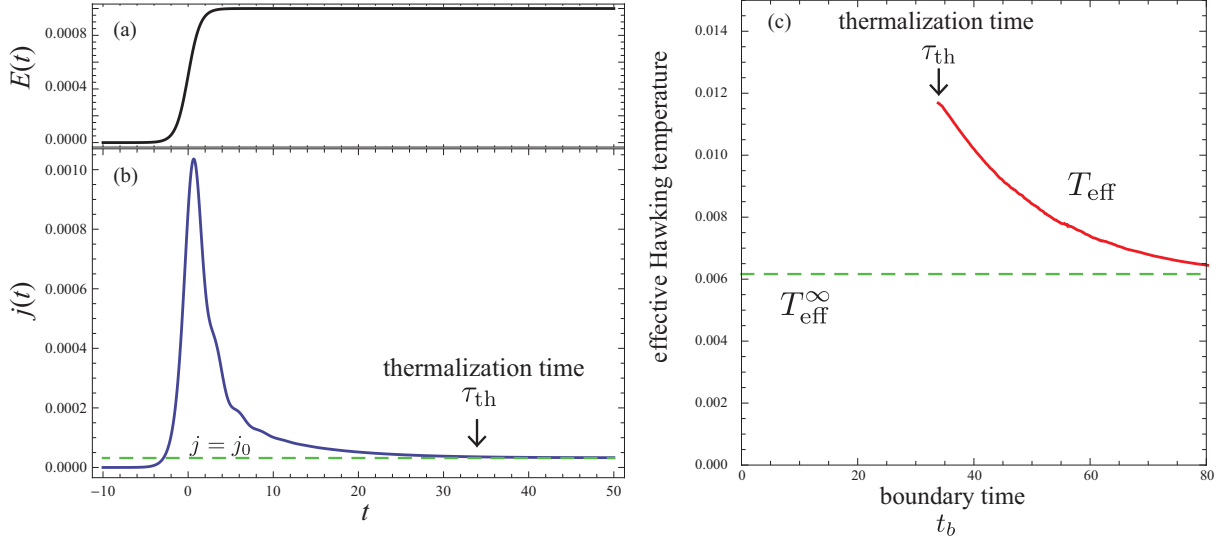


Figure 10: (a) The electric field $E(t)$. (b) Induced current $j(t)$. It converges to the steady state value $j = j_0$ (2.15). (c) The effective Hawking temperature (5.7) plotted against the boundary time. The “thermalization time” is defined as the boundary time of the horizon formation. In the long time limit, T_{eff} converges to the steady state value T_{eff}^{∞} . Same parameters as Fig. 9 is used.

formation of the horizon starts to affect the physics of the boundary only after its earliest boundary time (minimum of $t_b = t_{\text{AH}} + z_{\text{AH}}$) is reached. We call this time the “thermalization time” τ_{th} .

The time evolution of the current is shown in Fig. 10 (b). Initially, the current shows a large peak, and then relaxes to the steady state value j_0 . The initial peak is due to vacuum polarization, *i.e.*, the electric field pulls the quark antiquark pairs apart and the vacuum becomes polarized. This is better understood in the gapped case ($\eta \neq 0$) where the integral of the initial current peak is related to the induced vacuum polarization via $\int_0^{\infty} j(t)dt = P(E)$, *c.f.*, (1.3). However, in the gapless case this integral is ill defined and diverges since the current relaxes to a nonzero value $j = j_0$.

Figure 10 (c) shows the time evolution of the effective Hawking temperature T_{eff} plotted against the boundary time. In this example, T_{eff} emerges at the thermalization time $t = \tau_{\text{th}}$, and then quickly converges to the steady state value T_{eff}^{∞} . Although the true steady state is obtained when T_{eff} converges to T_{eff}^{∞} , the thermalization time $t = \tau_{\text{th}}$ captures the time scale of the whole relaxation process. Indeed, the value of the current seems to converge to the steady state value j_0 already around $t = \tau_{\text{th}}$ as seen in Fig. 10 (b).

The thermalization time is of particular interest in connection with experimental observations in RHIC and LHC that the QGP relaxes to the hydrodynamical regime

quite fast. In Fig. 11, we plot τ_{th} obtained for several processes with different parameters (the electric fields E and the AdS radius R corresponding to the coupling constant of the gauge theory). In the present gapless case, we expect that the thermalization time is related to the steady state effective Hawking temperature, which is the most prominent energy scale in the long time limit (the effect of the switch-on timescale ω should disappear by then). Indeed, by plotting τ_{th} against $1/z_p$ in Fig. 11 (b), we find a relation

$$\tau_{\text{th}} \sim a \frac{\hbar}{k_B T_{\text{eff}}^{\infty}}, \quad (5.15)$$

where a is a non-universal constant around $0.40/\pi$ in our numerical result. We have recovered the Planck constant (divided by 2π) \hbar and the Boltzmann constant k_B .

What is the physical meaning of the effective Hawking temperature that is induced by the electric field, and why does it govern the thermalization time scale?¹³ A hint comes from the condensed matter community, where similar physics has been studied in a zero temperature correlated system at a quantum critical point [9, 10]. When such systems are driven to a nonequilibrium state with finite current, many properties similar to finite temperature systems are observed. Using the Keldysh Green's function technique in a model of correlated electrons, it was demonstrated that the equations of motion of collective variables acquire a Langevin dissipation term with a Gaussian noise variable $\xi(x, t)$ that satisfies $\langle \xi(x, t) \xi(x', t') \rangle = \delta(x - x') \delta(t - t') 2T_{\text{eff}}^{\infty} / \gamma$ (γ is a model dependent parameter) [9]. This means that the system behaves as if it was coupled to a thermal bath with an effective temperature, in the present case, T_{eff}^{∞} . This gives a quantum field theory picture for our findings in the gravity dual description; The effective Hawking temperature is the dual of the nonequilibrium-induced Gaussian noise and acts as a source of decoherence and relaxation, which was explicitly studied by Sonner and Green [63]. Formula (5.15) relates the relaxation time scale to the effective temperature via two natural unit constants \hbar and k_B . We call this time scale the *Planckian thermalization time*, which becomes shorter (accelerated) as the electric field becomes stronger. A similar relation was discussed (although it was not proven) in Ref. [64] in the context of equilibrium Hi-Tc superconductors where the relaxation time was related to the inverse of the transition temperature T_c . The expression $\hbar/k_B T$ gives the shortest possible relaxation time scale and is realized when ‘‘Planckian dissipation’’ happens, *i.e.*, when no other time scale exists as in a conformal field theories (quantum critical point) coupled to a heat bath. The present situation is a nonequilibrium version

¹³One possibility is the Unruh effect [62]. In a system with charged particles accelerated by the electric fields, the Unruh effect may lead to an induced effective temperature $T_{\text{Unruh}} = \hbar b / 2\pi c k_B$, where b is the acceleration and c is the speed of light. However, in the present massless case, the speed of excitations do not change, *i.e.*, they are fixed to the speed of light. Thus, it is difficult to relate Unruh effect to the present system.

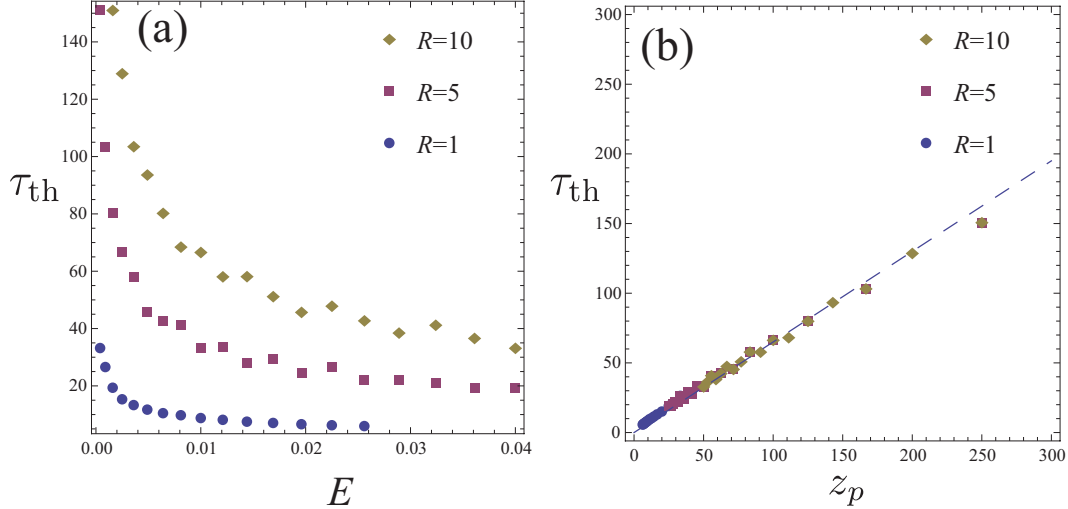


Figure 11: Thermalization time τ_{th} obtained for several processes with different field strengths and radius $R = 1, 5, 10$. The quench speed is fixed to $\omega = 4$. In (a), it is plotted against the field strength, and in (b) against the Planckian time scale z_p . An overlap takes place in (b), where the dashed line denotes the relation (5.15).

of the Planckian dissipation where the source of dissipation is provided by the induced Gaussian noise (= fluctuation that is characterized by the effective Hawking temperature) as explained above.

In the present system, the field induced Planckian time can be very short when the strength of the electric field becomes strong. This can be relevant in explaining the fast thermalization problem in RHIC and LHC. Of course, in reality, the hadrons are in the confined phase of QCD, while our real time calculation is done in the gapless deconfined phase of a supersymmetric QCD. However, when the external color electric field is stronger than all the other energy scales, we expect that (5.15) still sets the thermalization time. Let us estimate the induced Planckian time; Formula (5.15) can be rewritten as ($d = 0$, $\eta = 0$)

$$\tau_{\text{th}} \sim a\pi \left(\frac{\lambda}{2\pi^2} \right)^{1/4} \frac{\hbar}{k_B} E^{-1/2}. \quad (5.16)$$

The typical field strength realized in RHIC is $E = 10^4$ [MeV²] [1, 65, 66, 67, 68]. The string tension is an $\mathcal{O}(10)$ constant, which we set here to be $\lambda = 10$, $\hbar/k_B = 4\pi \times 6.08 \times 10^{-13}$ Ks (4π times the universal shear viscosity [69]) and $300\text{fm}/c \sim 10^{-21}$ s. Thus, we obtain,

$$\tau_{\text{th}} \sim 1 \text{ [fm}/c]. \quad (5.17)$$

This is of the same order of magnitude, compared to the upper bound of the thermalization time $1\text{fm}/s$ obtained from hydrodynamic analysis of QGP in RHIC [70].

However, in spite of this agreement, we must note that the present result cannot be the whole story. The calculation is based on the D3/D7 model in the probe limit. This means that only the quark dynamics is considered and the gluons are always in the thermal state (zero temperature in this case). In order to go further, we must consider gluon dynamics by including backreaction in the gluon sector.

From the viewpoint of dimension analysis, (5.16) is the simplest expression to obtain a time scale from the field strength. We expect that it gives the universal lower bound for the thermalization time scale in QGP production triggered by an external electric field. In addition, our finding suggests that QGP may reach the hydrodynamic regime in the presence of the field and *not* after it is lost. The hydrodynamic state is a nonequilibrium one with finite current, and the relaxation to this state may be accelerated by the fluctuation characterized by the effective Hawking temperature. The duration of the electric field [68] should be long enough to observe this effect.

In addition, there are other calculations of the thermalization in AdS/CFT which attempt to provide an explanation of the early thermalization from a different viewpoint, see for example Ref. [71] for an early work. One needs a more detailed comparison to our calculation.

6. Conclusion and discussions

In this paper we studied the vacuum decay process in the $\mathcal{N} = 2$ supersymmetric QCD at the strong coupling limit and in the large N_c limit via gauge/gravity duality. The decay is induced by strong electric fields which the quark hypermultiplet feels. We have derived the effective nonlinear electromagnetism Lagrangian which is known as an Euler-Heisenberg Lagrangian in constant background electric field to its full order in strong coupling gluons, and also derived the imaginary part of the effective Lagrangian that gives the vacuum decay rate. This is possible because the effective Lagrangian can be expressed as the D-brane's DBI action.

We also calculated the time-dependent response of the system once we apply a time-dependent electric field. When there is no mass gap, we find that the system evolves to a nonequilibrium stationary system with a constant electric current, in a time-dependent way. The thermalization time scale is calculated via the gauge/gravity duality, and the thermalization time-scale is found to be the Planckian time where the temperature is that of the final stationary state.

It is interesting that the calculated imaginary part of the effective Lagrangian for the constant electric field coincides with that of the ordinary QED, at the leading and sub-leading order in the large E expansion. This is a strange coincidence in the sense that our calculation of course includes all-order gluon effect at the leading large 't Hooft coupling, while in QED there is no gluon.

We finally discuss a relation between our calculations of the imaginary part and the holographic Schwinger effect studied in Ref. [26]. In Ref. [26], a direct generalization of the Schwinger instanton calculation of QED to strongly coupled $\mathcal{N} = 4$ supersymmetric Yang-Mills theory was presented. There, instead of the electron loop in a Euclidean spacetime for QED for the instanton calculation, one considers a string worldsheet in the $AdS_5 \times S^5$ geometry, with a probe D3-brane on which a constant electric field lives. The computation is, as in the case of the standard Schwinger calculations, valid at weak background electric field $E \ll m_W^2$ where m_W is the W-boson mass appearing in the Coulomb branch of the $\mathcal{N} = 4$ supersymmetric Yang-Mills theory. The result is, surprisingly, identical to the original Schwinger’s result, with a production rate

$$\Gamma_{\text{open string}} \sim \exp \left[-\pi \frac{m_{\text{eff}}(E)^2}{E} \right], \quad (6.1)$$

where the renormalized mass is

$$m_{\text{eff}}(E) = m_W - \frac{1}{2} A \frac{E}{m_W} \quad (6.2)$$

with $A = \sqrt{\lambda}/\pi$. Note that this expression agrees with the proposed all loop expression of QED effective Lagrangian for the single instanton case discussed in Refs. [72, 73, 74] (also described in Ref. [20]).

If we had studied the pair production process in a similar manner for our case, we expect the same result as the holographic Schwinger effect in Ref. [26], with $m_q = m_W$, because the separated D3-brane in Ref. [26] is just replaced by our flavor D7-brane. Thus, the expression (6.1) is also valid in our $\mathcal{N} = 2$ supersymmetric QCD. If we plot the production rate in the string and D-brane sectors we find a contradictory-looking fact; the worldsheet instanton (6.1) gives a nonzero production rate for any small E , while our calculation using the D-brane action (4.5) has a critical electric field below which the production rate vanishes.

The resolution of this “puzzle” is as follows: the true decay rate should be given by a function which smoothly connects the two solutions. This is because both calculations actually evaluate the same disk partition function, but in different limits. The holographic Schwinger effect (6.1) based on the disk amplitude evaluated in the AdS_5 is valid only at weak electric field. When electric field

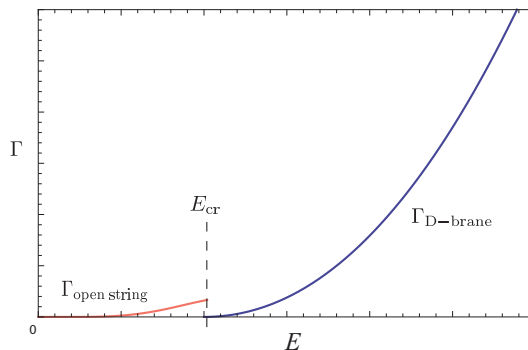


Figure 12: Schematic plot of the vacuum decay rate (production rate) obtained from the open string calculation [26] and from the D-brane calculation (4.5). The true decay rate should be a function which smoothly connects the two lines.

is weak, the area of the worldsheet instanton is large, and cannot be captured by its flat-space analogue at which any disk would be stabilized to a flat small one. On the other hand, the Dirac-Born-Infeld action which we used in this paper is based on a disk amplitude with a flat and small disk worldsheet. In the AdS_5 geometry, the small disk is realized in the large electric field limit as worldsheet instantons, so our DBI analysis is valid at large E . So, the two expressions come from the same single disk partition function with E vertex operator insertions, but in different limits.

To gain more insight on the interplay between the two limits, in Fig. 12 we plot the two contributions in a single plot. For small E , the string result (6.1) gives a nonzero but exponentially suppressed production rate, while at large E , we have a power-law large imaginary part. We expect that the whole behavior would be a smooth combination of the two lines.

We have seen in section 4 that our result of the imaginary part of the Lagrangian reproduces the leading and sub-leading behavior of the QED Schwinger effect calculations. How can it be consistent with (6.1)? In fact, the agreement which we found in section 4 is not really (6.1) but a different exponent, $m^2/(\sqrt{\lambda}E)$. See eq. (4.10) where one finds $E_{cr} \sim m^2/\sqrt{\lambda}$, instead of m^2 in (6.1). Since the gauge/gravity duality is valid at the large 'tHooft coupling constant λ , the holographic Schwinger effect (6.1) has a much more suppression than what we found in section 4, by the factor $\sqrt{\lambda}$ in the exponent.

There is another lesson which we can learn from the holographic Schwinger effect (6.1). A natural question arising in our derivation of the imaginary part is: why could we get the imaginary part by a classical action (string disk amplitude) rather than quantum loops? In fact, in the evaluation in a flat target spacetime in string theory, the imaginary part came from a cylinder amplitude which is a quantum loop [56, 57, 24, 25]. We can find a resolution of this counter-intuitive fact, by looking at the holographic Schwinger effect [26]. In the gauge/gravity duality, one replaces the N_c D3-branes by the AdS_5 geometry. Removing the D3-branes means that one needs to cap off one boundary of the cylinder, so it results in a disk worldsheet, that is, a classical DBI action. So, we learn that the reason why the classical DBI action can give the imaginary part is the gauge/gravity duality.

Finally, it is obvious that we have many future directions to extend our way to calculate the instability and the full Euler-Heisenberg action for strongly coupled systems. We would like to report on further applications elsewhere.

Acknowledgments

K.H. is indebted to Hiroshi Ooguri for valuable discussions and comments which were indispensable for finishing this work. K.H. would also like to thank K. Fukushima, G. Semenoff, H. Suganuma and S. Sugimoto for discussions. K.H. is grateful to the hospitality of Caltech theory group, and APCTP. T.O. acknowledges Y. Hidaka and

S. Sasaki for insightful discussions. K.H. and T.O. are partly supported by the Japan Ministry of Education, Culture, Sports, Science and Technology. This research was partially supported by the RIKEN iTHES project.

A. The imaginary action at zero temperature

Our result (3.9) for the gapless system is a bit complicated, so here we perform some more calculations for a simpler $T = 0$ case. We set $z_H = \infty$, then (3.9) becomes

$$\text{Im}\mathcal{L} = 2\pi^2\mu_7 \int_{R/\sqrt{2\pi\alpha'E}}^{\infty} dz \frac{R^8}{z^5} \sqrt{\left(\frac{(2\pi\alpha'E)^2}{R^4}z^4 - 1\right) \left(1 + \frac{z^6}{R^4}d^2\right)^{-1}}. \quad (\text{A.1})$$

To see the dependence in physical quantities, we change the integration coordinate as

$$z^2 = \frac{R^2}{2\pi\alpha'E} \frac{1}{x}, \quad (\text{A.2})$$

to obtain

$$\text{Im}\mathcal{L} = \pi^2\mu_7 \frac{(2\pi\alpha'E)^2}{R^4} \int_0^1 dx x^{3/2} \sqrt{\frac{1-x^2}{x^3 + d^2R^2/(2\pi\alpha'E)^3}}. \quad (\text{A.3})$$

From this expression, we can see that, for a given electric field, a larger charge density means a smaller magnitude of the imaginary part. This is counter-intuitive. In fact, when the imaginary part is zero, the electric current is given by (2.17) which shows a larger current for a larger density d . So, the d -dependence of the instability does not directly relate to the d -dependence of the electric current j .

To see this fact in more detail, we perform a small d expansion of the two quantities: $\text{Im}\mathcal{L}$ and the current j . First, we have

$$\text{Im}\mathcal{L} = \frac{\pi}{4}\mu_7 \frac{(2\pi\alpha'E)^2}{R^4} \left[1 - \frac{4c}{\pi} d^{2/3} \frac{R^{2/3}}{2\pi\alpha'E} + \text{higher order in } d \right], \quad (\text{A.4})$$

with a numerical coefficient $c \simeq 0.862$. On the other hand, the current j can be expanded for small density d as

$$j = \frac{(2\pi\alpha'E)^{3/2}}{R} \left[1 + \frac{1}{2} \frac{R^2}{(2\pi\alpha'E)^3} d^2 + \text{higher order in } d \right]. \quad (\text{A.5})$$

The dependence for small d is totally different.

Normally, a larger instability would lead to a larger current as a consequence of the vacuum breakdown. However, here in our supersymmetric QCD at strong coupling, the situation is not that intuitive.

B. The induced metric and the volume

In this appendix, we present the calculation of the induced metric on the D7-brane under the time-dependent electric field, studied in Sec. 5. We derive eq. (5.8) and eq. (5.9). Furthermore, we shall derive the effective Hawking temperature (5.13) by using the induced metric. (See for example Refs. [61, 63] for a similar calculation for a D3D5 steady system.)

The induced metric in the absence of the electric field on the D7-brane is

$$P[g]_{\mu\nu} = \frac{R^2}{z^2} \eta_{\mu\nu}, \quad P[g]_{zz} = \frac{R^2}{z^2}, \quad P[g]_{IJ} = R^2 G_{IJ}^{S^3}. \quad (\text{B.1})$$

The D7-brane action includes $\det(P[g] + 2\pi\alpha'F)$, and we expand it around a time-dependent electric field background. Defining the background F_{ab} plus the original induced metric $P[g]_{ab}$ as M_{ab} ,

$$M_{ab} \equiv P[g]_{ab} + 2\pi\alpha'F_{ab}^{\text{sol}}, \quad (\text{B.2})$$

and denote the fluctuation field strength as just δF_{ab} , then

$$\begin{aligned} & \sqrt{-\det(M + 2\pi\alpha'\delta F)} \\ &= \sqrt{-\det M} \left[1 + \frac{(2\pi\alpha')^2}{8} \left((\text{tr}[M^{-1}\delta F])^2 - 2\text{tr}[M^{-1}\delta F M^{-1}\delta F] \right) + \mathcal{O}((\delta F)^3) \right]. \end{aligned}$$

Here, we kept δF to its second order, and the first order fluctuation vanishes due to the fact that we are expanding around a classical solution.

Now, note that M^{-1} includes an anti-symmetric part as well as a symmetric part. We decompose it as $M^{-1} \equiv (M^{-1})^s + (M^{-1})^a$, where ‘‘s’’ and ‘‘a’’ mean symmetric and antisymmetric components, respectively. Then, assuming that the background solution depends only on t and z and also that the background field strength is nonzero only with the components F_{01} , F_{0z} and F_{1z} , we can simplify the fluctuation algebraically as

$$\sqrt{-\det(M + 2\pi\alpha'\delta F)} \Big|_{\mathcal{O}((\delta F)^2)} = -\sqrt{-\det M} \frac{(2\pi\alpha')^2}{4} \text{tr}[(M^{-1})^s \delta F (M^{-1})^s \delta F].$$

The front factor can be decomposed as

$$\sqrt{-\det M} = \sqrt{-\det((M^{-1})^s)^{-1}} \times \gamma, \quad \gamma \equiv \sqrt{\det(1 + ((M^{-1})^s)^{-1}(M^{-1})^a)}. \quad (\text{B.3})$$

So, writing

$$G_{ab} \equiv \mu_7^{1/2} \gamma^{1/2} (2\pi\alpha') \left[((M^{-1})^s)^{-1} \right]_{ab}, \quad (\text{B.4})$$

we obtain the fluctuation Lagrangian as

$$-\mu_7 \sqrt{-\det(M + 2\pi\alpha'\delta F)} \Big|_{\mathcal{O}((\delta F)^2)} = \frac{1}{4} \sqrt{-\det G} \text{tr}[G^{-1} \delta F G^{-1} \delta F]. \quad (\text{B.5})$$

This is nothing but the standard Maxwell Lagrangian, so this G given by eq. (B.6) can be regarded as a metric which the gauge fluctuation feels.

Once the effective metric G is derived, the volume element (5.8) which is necessary to calculate the location of the apparent horizon can be easily obtained. Here we present the explicit form of the effective metric G_{ab} . First, the $(0, 1, z)$ sector of the metric is

$$G = \frac{R^2}{z^2} \begin{pmatrix} -1 + a^2 + b^2 & bc & -ac \\ bc & 1 - a^2 + c^2 & -ab \\ -ac & -ab & 1 - b^2 + c^2 \end{pmatrix} \quad (\text{B.6})$$

where

$$a \equiv 2\pi\alpha' \frac{z^2}{R^2} F_{01}, \quad b \equiv 2\pi\alpha' \frac{z^2}{R^2} F_{0z}, \quad c \equiv 2\pi\alpha' \frac{z^2}{R^2} F_{1z}. \quad (\text{B.7})$$

The $(2, 3)$ sector is

$$G = \frac{R^2}{z^2} \begin{pmatrix} 1 & 0 \\ 0 & 1 \end{pmatrix}, \quad (\text{B.8})$$

and the S^3 sector is given by $G_{IJ} = R^2 G_{IJ}^{\text{unit } S^3}$.

From this formula for the induced metric, let us obtain an explicit expression of the metric for the nonequilibrium steady state with the electric current considered in section 2. This can derive the effective Hawking temperature (5.13). For simplicity, we take $d = 0$ (vanishing charge density) and $T = 0$ (zero temperature for the bulk gluons). The configuration of section 2 provides

$$a = \frac{z^2}{z_p^2}, \quad b = 0, \quad c = \frac{R^2 z}{z_p^3} \sqrt{\frac{1 - z^4/z_p^4}{1 - z^6/z_p^6}}. \quad (\text{B.9})$$

The nontrivial $(0, z)$ components of the effective metric G (B.6) is given as

$$ds^2 = \frac{R^2}{z^2} \left((-1 + a^2) dt^2 - 2ac dt dz + (1 + c^2) dz^2 \right). \quad (\text{B.10})$$

We can diagonalize this metric by the following field redefinition (see for example a similar transformation in Ref. [63])

$$t' \equiv t + \int^z dz \frac{ac}{1 - z^2} \quad (\text{B.11})$$

to obtain

$$ds^2 = \frac{R^2}{z^2} \left((-1 + a^2) dt'^2 + \frac{-1 + a^2 - c^2}{-1 + a^2} dz^2 \right). \quad (\text{B.12})$$

Substituting (B.9) and expanding the metric around z_p as $z = z_p + \delta z$ (here $\delta z < 0$),

$$ds^2 = \frac{R^2}{z_p^2} \left(-\frac{2|\delta z|}{z_p} dt'^2 + \frac{z_p}{|\delta z|} [d(\delta z)]^2 \right). \quad (\text{B.13})$$

This metric is nothing but a near-horizon metric of a black hole. So we can actually see that the mesons on the D7-brane feels a metric with an event horizon.

Using a redefinition to a radial r coordinate, $|\delta z| \equiv (3z_p/4R^2)r^2$, and Euclideanize the time direction t' and imposing the smoothness condition of the metric, we obtain the periodicity

$$it' \sim it' + 2\pi z_p \sqrt{2/3}. \quad (\text{B.14})$$

So the Hawking temperature calculated from the induced metric is given by

$$T_{\text{eff}} = \sqrt{\frac{3}{8}} \frac{1}{\pi z_p}. \quad (\text{B.15})$$

This is the effective temperature which the mesons feel, in the stationary nonequilibrium case, (5.13). In section 5, we have defined a time-dependent version of the effective temperature (5.7), by just generalizing (5.13). The definition of (5.7) uses the apparent horizon, so it is a natural choice, among ones which converges to (5.13) at later time.

References

- [1] D. E. Kharzeev, L. D. McLerran, and H. J. Warringa, *The Effects of topological charge change in heavy ion collisions: 'Event by event P and CP violation'*, *Nucl.Phys.* **A803** (2008) 227–253, [[arXiv:0711.0950](#)].
- [2] K. Yagi, T. Hatsuda, and Y. Miake, *Quark-Gluon Plasma*. Cambridge University Press, 2005.
- [3] F. Gelis, E. Iancu, J. Jalilian-Marian, and R. Venugopalan, *The Color Glass Condensate*, *Ann.Rev.Nucl.Part.Sci.* **60** (2010) 463–489, [[arXiv:1002.0333](#)].
- [4] T. Lappi and L. McLerran, *Some features of the glasma*, *Nucl.Phys.* **A772** (2006) 200–212, [[hep-ph/0602189](#)].
- [5] T. Oka and H. Aoki, *Ground-State Decay Rate for the Zener Breakdown in Band and Mott Insulators*, *Physical Review Letters* **95** (Sept., 2005) 1–4.
- [6] T. Oka, and H. Aoki, *Nonequilibrium Quantum Breakdown in a Strongly Correlated Electron System, Quantum and Semi-classical Percolation & Breakdown (Lecture N* (2008).

- [7] T. Oka R. Arita and H. Aoki, *Breakdown of a Mott insulator – non-adiabatic tunneling mechanism*, *Phys.Rev.Lett.* **91** (2003) 66406.
- [8] M. Eckstein, T. Oka, and P. Werner, *Dielectric Breakdown of Mott Insulators in Dynamical Mean-Field Theory*, *Physical Review Letters* **105** (Sept., 2010).
- [9] A. Mitra, S. Takei, Y. B. Kim, and A. J. Millis, *Nonequilibrium Quantum Criticality in Open Electronic Systems*, *Phys. Rev. Lett.* **97** (2006) 236808.
- [10] A. Mitra and A. Millis, *Current-driven quantum criticality in itinerant electron ferromagnets*, *Physical Review B* **77** (June, 2008) 220404.
- [11] D. Dalidovich and P. Phillips, *Nonlinear transport near a quantum phase transition in two dimensions*, *Phys. Rev. Lett.* **93** (2004) 27004.
- [12] A. Karch and S. L. Sondhi, *Non-linear, finite frequency quantum critical transport from AdS/CFT*, *Journal of High Energy Physics* **2011** (Jan., 2011) 16, [arXiv:1008.4134].
- [13] A. G. Green and S. L. Sondhi, *Nonlinear Quantum Critical Transport and the Schwinger Mechanism for a Superfluid-Mott-Insulator Transition of Bosons*, *Phys. Rev. Lett.* **95** (2005) 267001.
- [14] J. M. Maldacena, *The Large N limit of superconformal field theories and supergravity*, *Adv.Theor.Math.Phys.* **2** (1998) 231–252, [hep-th/9711200].
- [15] S. Gubser, I. R. Klebanov, and A. M. Polyakov, *Gauge theory correlators from noncritical string theory*, *Phys.Lett.* **B428** (1998) 105–114, [hep-th/9802109].
- [16] E. Witten, *Anti-de Sitter space and holography*, *Adv.Theor.Math.Phys.* **2** (1998) 253–291, [hep-th/9802150].
- [17] W. Heisenberg and H. Euler, *Folgerungen aus der Diracschen Theorie des Positrons*, *Z. Physik* **98** (1936), no. 1 714–732.
- [18] V. Weisskopf, *The electrodynamics of the vacuum based on the quantum theory of the electron*, *Kong. Dans. Vid. Selsk. Math-fys. Medd. XIV No. 6 (1936)*; English translation in: *Early Quantum Electrodynamics: A Source Book*, A. I. Miller, (Cambridge University Press, 1994). (1936).
- [19] J. Schwinger, *On Gauge Invariance and Vacuum Polarization*, *Phys. Rev.* **82** (1951) 664.
- [20] G. V. Dunne, *Heisenberg-Euler Effective Lagrangians : Basics and Extensions*, 0406216.
- [21] W. Dittrich and H. Gies, *Probing the Quantum Vacuum*. Springer-Verlag, Berlin, 2000.

- [22] S. Coleman, *More about the massive Schwinger model*, *Annals of Physics* **101** (Sept., 1976) 239–267.
- [23] A. Karch and E. Katz, *Adding flavor to AdS / CFT*, *JHEP* **0206** (2002) 043, [[hep-th/0205236](#)].
- [24] C. Bachas and M. Porrati, *Pair creation of open strings in an electric field*, *Physics Letters B* **296** (Dec., 1992) 77–84.
- [25] C. Bachas, *D-brane dynamics*, *Phys.Lett.* **B374** (1996) 37–42, [[hep-th/9511043](#)].
- [26] G. W. Semenoff and K. Zarembo, *Holographic Schwinger Effect*, *Physical Review Letters* **107** (Oct., 2011) 171601.
- [27] E. S. Fradkin and A. A. Tseytlin, *Nonlinear Electrodynamics From Quantized Strings*, *Phys.Lett.B* **163** (1985) 123.
- [28] K.-Y. Kim, S.-J. Sin, and I. Zahed, *Dense and Hot Holographic QCD: Finite Baryonic E Field*, *JHEP* **0807** (2008) 096, [[arXiv:0803.0318](#)].
- [29] S. R. Das, T. Nishioka, and T. Takayanagi, *Probe Branes, Time-dependent Couplings and Thermalization in AdS/CFT*, *JHEP* **1007** (2010) 071, [[arXiv:1005.3348](#)].
- [30] K. Hashimoto, N. Iizuka, and T. Oka, *Rapid Thermalization by Baryon Injection in Gauge/Gravity Duality*, *Phys.Rev.* **D84** (2011) 066005, [[arXiv:1012.4463](#)].
- [31] U. H. Danielsson, E. Keski-Vakkuri, and M. Kruczenski, *Black hole formation in AdS and thermalization on the boundary*, *JHEP* **0002** (2000) 039, [[hep-th/9912209](#)].
- [32] S. Bhattacharyya and S. Minwalla, *Weak Field Black Hole Formation in Asymptotically AdS Spacetimes*, *JHEP* **0909** (2009) 034, [[arXiv:0904.0464](#)].
- [33] R. A. Janik and R. B. Peschanski, *Gauge/gravity duality and thermalization of a boost-invariant perfect fluid*, *Phys.Rev.* **D74** (2006) 046007, [[hep-th/0606149](#)].
- [34] H. Ebrahim and M. Headrick, *Instantaneous Thermalization in Holographic Plasmas*, [arXiv:1010.5443](#).
- [35] J. Abajo-Arrastia, J. Aparicio, and E. Lopez, *Holographic Evolution of Entanglement Entropy*, *JHEP* **1011** (2010) 149, [[arXiv:1006.4090](#)].
- [36] V. Balasubramanian, A. Bernamonti, J. de Boer, N. Copland, B. Craps, et al., *Thermalization of Strongly Coupled Field Theories*, *Phys.Rev.Lett.* **106** (2011) 191601, [[arXiv:1012.4753](#)].
- [37] A. Buchel, L. Lehner, and R. C. Myers, *Thermal quenches in $N=2^*$ plasmas*, *JHEP* **1208** (2012) 049, [[arXiv:1206.6785](#)].
- [38] M. P. Heller, D. Mateos, W. van der Schee, and D. Trancanelli, *Strong Coupling Isotropization of Non-Abelian Plasmas Simplified*, *Phys.Rev.Lett.* **108** (2012) 191601, [[arXiv:1202.0981](#)].

- [39] V. Balasubramanian, A. Bernamonti, J. de Boer, B. Craps, L. Franti, et al., *Inhomogeneous Thermalization in Strongly Coupled Field Theories*, [arXiv:1307.1487](#).
- [40] A. Buchel, L. Lehner, R. C. Myers, and A. van Niekerk, *Quantum quenches of holographic plasmas*, *JHEP* **1305** (2013) 067, [[arXiv:1302.2924](#)].
- [41] A. Buchel, R. C. Myers, and A. van Niekerk, *Universality of Abrupt Holographic Quenches*, [arXiv:1307.4740](#).
- [42] J. Ambjorn and Y. Makeenko, *Remarks on Holographic Wilson Loops and the Schwinger Effect*, *Phys.Rev.* **D85** (2012) 061901, [[arXiv:1112.5606](#)].
- [43] S. Bolognesi, F. Kiefer, and E. Rabinovici, *Comments on Critical Electric and Magnetic Fields from Holography*, *JHEP* **1301** (2013) 174, [[arXiv:1210.4170](#)].
- [44] Y. Sato and K. Yoshida, *Holographic description of the Schwinger effect in electric and magnetic fields*, *JHEP* **1304** (2013) 111, [[arXiv:1303.0112](#)].
- [45] Y. Sato and K. Yoshida, *Potential Analysis in Holographic Schwinger Effect*, [arXiv:1304.7917](#).
- [46] Y. Sato and K. Yoshida, *Holographic Schwinger effect in confining phase*, [arXiv:1306.5512](#).
- [47] A. Karch and A. O’Bannon, *Metallic AdS/CFT*, *JHEP* **0709** (2007) 024, [[arXiv:0705.3870](#)].
- [48] T. Albash, V. G. Filev, C. V. Johnson, and A. Kundu, *Quarks in an external electric field in finite temperature large N gauge theory*, *JHEP* **0808** (2008) 092, [[arXiv:0709.1554](#)].
- [49] J. Erdmenger, N. Evans, I. Kirsch, and E. Threlfall, *Mesons in Gauge/Gravity Duals - A Review*, *Eur.Phys.J.* **A35** (2008) 81–133, [[arXiv:0711.4467](#)].
- [50] O. Bergman, G. Lifschytz, and M. Lippert, *Response of Holographic QCD to Electric and Magnetic Fields*, *JHEP* **0805** (2008) 007, [[arXiv:0802.3720](#)].
- [51] C. V. Johnson and A. Kundu, *External Fields and Chiral Symmetry Breaking in the Sakai-Sugimoto Model*, *JHEP* **0812** (2008) 053, [[arXiv:0803.0038](#)].
- [52] A. Karch and A. O’Bannon, *Holographic thermodynamics at finite baryon density: Some exact results*, *JHEP* **0711** (2007) 074, [[arXiv:0709.0570](#)].
- [53] J. Erdmenger, R. Meyer, and J. P. Shock, *AdS/CFT with flavour in electric and magnetic Kalb-Ramond fields*, *JHEP* **0712** (2007) 091, [[arXiv:0709.1551](#)].
- [54] C. Herzog, A. Karch, P. Kovtun, C. Kozcaz, and L. Yaffe, *Energy loss of a heavy quark moving through $N=4$ supersymmetric Yang-Mills plasma*, *JHEP* **0607** (2006) 013, [[hep-th/0605158](#)].

- [55] S. S. Gubser, *Drag force in AdS/CFT*, *Phys.Rev.* **D74** (2006) 126005, [[hep-th/0605182](#)].
- [56] C. P. Burgess, *Open string instability in background electric fields*, *Nucl.Phys.* **B294** (1987) 427.
- [57] V. V. Nesterenko, *The dynamics of open strings in a background electromagnetic field*, *Int.J.Mod.Phys.* **A4** (1989) 2627–2652.
- [58] M. Bianchi, D. Z. Freedman, and K. Skenderis, *Holographic renormalization*, *Nucl.Phys.* **B631** (2002) 159–194, [[hep-th/0112119](#)].
- [59] A. Karch, A. O’Bannon, and K. Skenderis, *Holographic renormalization of probe D-branes in AdS/CFT*, *JHEP* **0604** (2006) 015, [[hep-th/0512125](#)].
- [60] M. Kruczenski, D. Mateos, R. C. Myers, and D. J. Winters, *Meson spectroscopy in AdS / CFT with flavor*, *JHEP* **0307** (2003) 049, [[hep-th/0304032](#)].
- [61] K.-Y. Kim, J. P. Shock, and J. Tarrío, *The open string membrane paradigm with external electromagnetic fields*, *JHEP* **1106** (2011) 017, [[arXiv:1103.4581](#)].
- [62] W. G. Unruh, *Notes on black-hole evaporation*, *Phys. Rev. D* **14** (1976) 870.
- [63] J. Sonner and A. G. Green, *Hawking Radiation and Non-equilibrium Quantum Critical Current Noise*, *Phys.Rev.Lett.* **109** (2012) 091601, [[arXiv:1203.4908](#)].
- [64] J. Zaanen, *Superconductivity: why the temperature is high.*, *Nature* **430** (July, 2004) 512–3.
- [65] V. Skokov, A. Y. Illarionov, and V. Toneev, *Estimate of the magnetic field strength in heavy-ion collisions*, *Int.J.Mod.Phys.* **A24** (2009) 5925–5932, [[arXiv:0907.1396](#)].
- [66] V. Voronyuk, V. Toneev, W. Cassing, E. Bratkovskaya, V. Konchakovski, et al., *(Electro-)Magnetic field evolution in relativistic heavy-ion collisions*, *Phys.Rev.* **C83** (2011) 054911, [[arXiv:1103.4239](#)].
- [67] A. Bzdak and V. Skokov, *Event-by-event fluctuations of magnetic and electric fields in heavy ion collisions*, *Phys.Lett.* **B710** (2012) 171–174, [[arXiv:1111.1949](#)].
- [68] W.-T. Deng and X.-G. Huang, *Event-by-event generation of electromagnetic fields in heavy-ion collisions*, *Phys.Rev.* **C85** (2012) 044907, [[arXiv:1201.5108](#)].
- [69] P. Kovtun, D. Son, and A. Starinets, *Viscosity in Strongly Interacting Quantum Field Theories from Black Hole Physics*, *Physical Review Letters* **94** (Mar., 2005) 111601.
- [70] U. Heinz, *Thermalization at RHIC*, in *AIP Conference Proceedings*, vol. 739, pp. 163–180, AIP, Dec., 2004.
- [71] P. M. Chesler and L. G. Yaffe, *Horizon formation and far-from-equilibrium isotropization in supersymmetric Yang-Mills plasma*, *Phys.Rev.Lett.* **102** (2009) 211601, [[arXiv:0812.2053](#)].

- [72] V. I. Ritus, *Method Of Eigenfunctions And Mass Operator In Quantum Electrodynamics Of A Constant Field*, *Sov. Phys. JETP* **48** (1978) 788.
- [73] S. L. Lebedev and V. I. Ritus, *Virial Representation Of The Imaginary Part Of The Lagrange Function Of The Electromagnetic Field*, *Sov. Phys. JETP* **59** (1984) 237.
- [74] I. K. Affleck, O. Alvarez, and N. S. Manton, *Pair production at strong coupling in weak external fields*, *Nuclear Physics B* **197** (Apr., 1982) 509–519.